

**APPLICATION OF ISOTOPE MASS-BALANCE MODELS ($\delta^2\text{H}$, $\delta^{18}\text{O}$) TO ASSESS
SPATIAL VARIABILITY IN LAKE HYDROLOGY ON THE NORTHERN GREAT
PLAINS, CANADA**

H.A. Haig^{1,2}, N.M. Hayes^{1,3}, G.L. Simpson⁴, Y. Yi^{5,6}, B. Wissel⁴, K. Finlay⁷, K.R. Hodder⁸, and
P.R. Leavitt^{1,4,7,9,+}

¹Limnology Laboratory, Department of Biology, University of Regina, Regina, Saskatchewan
S4S 0A2, Canada

² Present address: Saskatchewan Water Security Agency, Regina, Saskatchewan, S4P 4K1,
Canada.

³ Present address: Biology Department, University of Wisconsin Stout, Menomonie, Wisconsin,
54751, USA

⁴ Institute of Environmental Change and Society, University of Regina, Regina, Saskatchewan
S4S 0A2, Canada

⁵ Environmental Monitoring and Science Division, Alberta Environment and Parks, Edmonton,
Alberta, T5J 5C6, Canada

⁶ Department of Geography, University of Victoria, Victoria, BC V8W 3R4, Canada

⁷ Department of Biology, University of Regina, Regina, SK S4S0A2, Canada;

⁸ Prairie Environmental Processes Laboratory, Department of Geography and Environmental
Studies, University of Regina, Regina, Saskatchewan, S4S 0A2, Canada

⁹ Institute of Global Food Security, Queen's University Belfast, Belfast, Co. Antrim, BT9 5DL,
United Kingdom

⁺corresponding author: p.leavitt@qub.ac.uk

37 **Highlights:**

- 38 • Water isotope mass budgets were calculated for 105 prairie lakes
- 39 • Inflow was regulated by rainfall not snow and exceeded evaporation in most lakes
- 40 • Landscape patterns of lake hydrology were unrelated to extant climatic gradients
- 41 • Rapid infiltration of precipitation in sandy soils may increase lake susceptibility to aridity

42

43 **Email and ORCID:**

44 HAH haig.a.heather@gmail.com, orcid.org/0000-0002-0208-8179

45 NMH hayesn@uwstout.edu, orcid.org/0000-0002-5664-9939

46 GLS Gavin.Simpson@uregina.ca, orcid.org/0000-0002-9084-8413

47 YY yiyi@uvic.ca, orcid.org/0000-0002-1403-9841

48 BW Bjoern.Wissel@uregina.ca, orcid.org/0000-0001-6312-149X

49 KF Kerri.Finlay@uregina.ca, <https://orcid.org/0000-0001-6835-8832>

50 KRH krhodder@gmail.com, orcid.org/0000-0002-1447-2557

51 PRL Peter.Leavitt@uregina.ca, P.Leavitt@qub.ac.uk, orcid.org/0000-0001-9805-9307

52 **Abstract**

53 Existing data on surface water availability and fluxes are limited in many areas across the
54 globe, making it difficult to predict effects of future climate variability at the landscape scale.
55 Here we used isotope mass balances (IMB) of hydrogen ($\delta^2\text{H}$) and oxygen ($\delta^{18}\text{O}$) in water from
56 105 prairie lakes to quantify and map spatial variation in lake hydrology and susceptibility to
57 climate in the Northern Great Plains (NGP) of Canada. Contrary to previous research following
58 an arid interval (2004), IBMs for a relatively wet period (2013) suggested that source waters for
59 most lakes were more isotopically-similar to rainfall than to snow. In addition, isotopically-
60 derived water balances showed that inflow exceeded evaporation in many basins, despite a
61 pronounced regional water deficit (potential evaporation > precipitation). Isotope-based
62 estimates of water yield and precipitation runoff coefficients calculated using the gross drainage
63 area of each lake showed that lakes were hydrological hotspots that concentrated surface runoff
64 even in endorheic basins. At the landscape scale, hydrological parameters demonstrated little
65 relationship with annual meteorological conditions, suggesting that basin-specific hydrology
66 could not be predicted easily from patterns of temperature or precipitation. Instead, principal
67 components analysis (PCA) and generalized additive models (GAMs) showed that local soil
68 characteristics, vegetation cover, and basin geomorphology were important controls of lake
69 hydrology and susceptibility to climate variability, with basins in catchments with sandy soils
70 and rapid infiltration likely to be impacted by increased aridity and reduced water inflows.

71 **Keywords:**

72 Water isotopes, climate, evaporation/inflow (E/I), catchment yield, runoff coefficient,
73 generalized additive models

74

1. Introduction

The hydrological sensitivity of the Northern Great Plains (NGP) to climate and land use change has been intensively studied (Coles et al., 2018; Khaliq et al, 2015; Pomeroy et al., 2007; van der Kamp et al., 1999). Nonetheless uncertainty remains regarding how climate, hydrological processes, and drainage basin characteristics interact to regulate precipitation transport to surface waterbodies (Shook et al., 2015). For example, runoff from large catchments with low topographic relief appears to accumulate in lakes of the NGP despite precipitation deficits of 200 – 600 mm year⁻¹ (LaBaugh et al., 1997; Pham et al., 2009; Winter and Change, 1998). Further, high inter-annual variability in runoff, combined with uncertainty in general circulation model predictions of the magnitude and severity of variation in seasonal precipitation, make it difficult to forecast how prairie lakes may respond to forthcoming climate change (Asong et al., 2016; Dibike et al. 2016). Traditionally, the sustainability of surface waters in the NGP has been assessed using long-term records of lake level and streamflow; however, most basins are rarely monitored, or completely ungauged, and additional methods are needed to improve our understanding of the mechanisms regulating transport of precipitation from catchments into lakes over large spatial scales (Gan and Tanzeeba, 2012; Jacques et al., 2014; van der Kamp et al., 2008).

Stable isotopes of hydrogen ($\delta^2\text{H}$) and oxygen ($\delta^{18}\text{O}$) have been proposed as a reliable means to quantify the water balance of lakes, including the study of how regional precipitation is transferred to lakes (Gibson, 2002a; Gibson et al., 2005, 2016a, 2016b). Common applications of water isotope analysis include estimation of the relative importance of individual source waters (Gao et al., 2018; Narancic et al., 2017; Turner et al., 2014; Yi et al., 2008), evaporation (E) to inflow (I) ratios (E/I) (Gibson and Edwards, 2002; Gibson and Reid, 2010, 2014), the volume of

98 ungauged surface runoff (Fekete et al., 2006; Gibson et al., 2015), the importance of infiltration
99 in wetlands (Bam and Ireson, 2019), and catchment water yield (Bennett et al., 2008; Gibson et
100 al., 2018). In particular, water isotope mass balances (IMB) provide a unique opportunity to trace
101 the water molecule itself, as transformation and fractionation processes are well understood, and
102 have been used for decades to track important processes throughout the water cycle (Craig et al.,
103 1965; Gat, 1995).

104 Winter precipitation is thought to be the predominant source of water for runoff to sustain
105 lakes in the NGP, particularly in conditions when runoff occurs over frozen soils (Carey and
106 Cole, 2013; Coles et al., 2017; Pomeroy, 2007, 2009; Shook et al., 2015). As a well-established
107 technique, IMB has been used in the NGP to quantify the relative importance of rain versus snow
108 in water budgets for 70 lakes during a multi-year period of aridity (2002-2004), with 72% of
109 basins relying mainly on snowmelt to sustain their water balance (Pham et al., 2009). However,
110 increased importance of rainwater in sustaining flow since 2010 has challenged the primacy of
111 snowpack in controlling NGP surface water balance (Dumanski et al., 2015; Haig et al., 2020;
112 Shook and Pomeroy, 2012). Given that some lakes have experienced marked declines in water
113 supply (van der Kamp et al., 2008), others have seen sharp increases in inflow (McCullough et
114 al., 2012), and that the NGP has experienced high variability in winter precipitation and runoff
115 during the past decade (Brimelow et al., 2014; Mahmood et al., 2017; Rodell et al., 2018), there
116 is a need to quantify the patterns and controls of spatial variability of grassland lake hydrology.
117 Further, a better understanding of the relative importance of winter and summer precipitation to
118 prairie lakes is essential to forecast how these ecosystems may respond to future climate change
119 (Asong et al., 2016; Bonsal et al., 2017).

Evaluation of the hydrological processes that regulate precipitation transfer from catchments into lentic or lotic systems requires extensive monitoring networks or models to estimate water yield and runoff coefficient (Bemrose et al., 2009; Bennett et al., 2008; Cole, 2013; Dumanski et al., 2015; Ehsanzadeh et al., 2012). Water yield (i.e., depth-equivalent runoff) provides a standard metric of water export from catchments, but contains little information on the source of water (Bemrose et al., 2009; Gibson et al., 2016, 2018). Drainage basin response to precipitation events can also be characterized by a runoff coefficient, calculated as % precipitation that falls on a catchment and contributes to lake inflow (Blume et al. 2007), although the process is known by other terms (e.g., response factor, runoff ratio, hydrological response, annual runoff coefficient). In most cases, insufficient data exist to quantify water yield and runoff coefficients for lakes, therefore hydrologists often extrapolate to lakes from estimates of gauged rivers, even though many prairie lakes and wetlands lack channelized inflow (Bam and Ireson, 2019; Bemrose et al., 2009; Pham et al. 2009). Fortunately, recent advances in the application of water IMBs have allowed investigators to approximate water yield for diverse catchments (Bennett et al., 2008; Gibson et al., 2010), although, to date, few studies have related isotopically-derived parameters of lake hydrology to the landscape characteristics which might regulate inflow (climatic, edaphic, vegetation, wetland, landuse, etc.) (e.g., Turner et al., 2014).

In this study, we analyzed water isotopes from over 100 prairie lakes in the NGP of central Canada to identify source waters, calculate water balance (E/I), quantify the transformation of catchment precipitation to lake inflow (water yield, runoff coefficient), and determine how these parameters vary over a large spatial scale (ca. 285,000 km²). First, lake-specific IMBs were calculated to assess the relative importance of snowmelt runoff and rainfall to each lake's water balance, and to estimate the isotope-derived ratio of evaporation to inflow (E/I). Second, E/I

ratios were used to estimate the volume of runoff, water yield (depth equivalent runoff), and runoff coefficients by incorporating both isotopic analysis and digital elevation models (DEM) of each catchment. Third, spatial patterns of all output parameters were mapped for the entire study area using generalized additive models (GAM) that account for non-linear changes in spatial gradients. Finally, principal component analysis (PCA) was used to explore basin characteristics that could be related to the spatial variation in lake hydrology. Based on a survey a decade earlier (Pham et al., 2009), we hypothesized that lakes would be sustained mainly by snowmelt water (Pomeroy et al., 2007), but that landscape gradients of evaporation (high in west, lower in east) (Bonsal and Shabbar 2008) would regulate spatial patterns of water balance and lake sensitivity to climate variability.

2. Methods

2.1 Site descriptions

In total, 105 study basins were selected to characterize the diversity of lentic hydrology over the Prairies of Saskatchewan, Canada, an area encompassing more than 285,000 km² of mixed-use grassland (Fig. 1). Regional climate is characterized as cool-summer humid continental (Köppen Dfb classification), with short summers (mean 19°C in July), cold winters (mean -16°C in January), and low annual temperatures (~1°C). Mean annual precipitation is ~380 mm, with most rain falling between May and July, and most runoff during the short snowmelt period of spring (Akinremi et al., 1999; Coles et al., 2017; Fang et al., 2007), and a pronounced long-term gradient in precipitation from drier in the west (moisture deficit of 600 mm year⁻¹) to wetter in the east (deficit 200 mm year⁻¹) (Martin, 2002; Pham et al., 2009). During the hydrological year of the survey (2013), mean annual precipitation in the study region was 348.3 mm (standard deviation, σ = 59.0, median, \tilde{x} = 333.5) and mean temperature during the open water (April-

166 October) season was 12.6 °C ($\sigma = 0.6$, $\bar{x} = 12.5$) (Environment and Climate Change Canada,
167 ECCC, <http://climate.weather.gc.ca>). Evaporation calculated using the Meyer's method was
168 810.9 mm ($\sigma = 90.6$), resulting in a mean water deficient for the entire study region of 462.6 mm
169 during 2013 ($\sigma = 110.9$) (Martin, 2002).

170 Land cover within each lakes' drainage basin was composed mainly of agricultural cropland
171 ($\mu \pm \sigma = 46.9 \pm 27.7$ %), grassland and pasture (28.1 ± 22.1 %), wetlands (3.3 ± 7.7 %),
172 permanent waterbodies (6.0 ± 5.6 %), tree cover (6.0 ± 14.6 %), shrub land (4.4 ± 8.8 %), or
173 urban developments (0.88 ± 2.1 %) (Agriculture and Agri-Food Canada, AAFC, 2013; Table 1).
174 Soil characteristics (e.g., sand content (%), hydraulic conductivity as cm h^{-1}) were determined for
175 each drainage basin using the Soil Landscapes of Canada dataset (version 3.2). Hydrological
176 characteristics of the basin were calculated from digital elevation model (DEM; see below) and
177 included the surface area of small depressions ('sinks'; m^2), the volume of the depressions (m^3),
178 basin shape (i.e., form factor; Zăvoianu 1985), average distance between streams (m), average
179 distance of overland flow (m), and drainage density (m^{-1}).

180 2.2 Field sampling

181 Survey lakes were sampled once in August 2013. Sites spanned a wide spatial extent of 4
182 ° latitude and 10 ° longitude (Fig. 1) and were selected to maximize geographic coverage
183 throughout the grasslands region of Saskatchewan while maintaining most of the 70 lakes
184 sampled in 2004 by Pham et al. (2009). Physical and chemical composition of lakes varied
185 greatly across the region and are summarized in Plancq et al. (2018). Briefly, water quality
186 characteristics exhibited a wide range of salinity (as total dissolved solids, TDS, 0.1 - 102 g L^{-1}),
187 mean ($\pm \sigma$) phytoplankton abundance (Chlorophyll-a, $\mu\text{g Chl a L}^{-1}$, 32.1 ± 115.5 , $\bar{x} = 8.5$), and
188 diverse ionic composition (e.g., SO_4 , mg L^{-1} , 6221.0 ± 15304.3 , $\bar{x} = 1152.1$). Sites were also

selected to cover a wide range in physical parameters such as lake depth (m, 6.5 ± 6.3 , $\bar{x} = 4.0$) and surface area (10^6 m^2 , 1.8 ± 6.4 , $\bar{x} = 0.3$) (Table 1). Most systems were polymictic, with only ~20 % of sites displaying some evidence of thermal or chemical stratification during the late-summer sampling period (Plancq et al., 2018).

2.3 Drainage basin delineation

Drainage areas were estimated for each lake to allow calculation of water yield and runoff coefficient. Here we developed a standardized procedure to identify gross drainage area (GDA) and sink-free drainage basin area (SFDA) using ArcHydro (ESRI, v2.1) and the Canadian Digital Elevation Model (CDEM, v1.1). Base resolution of the CDEM tiles is 0.75 arc seconds. Each tile was converted to a plane coordinate projection (20-m resolution) at the time of extraction. We modified the ESRI Terrain Pre-processing Workflow UC4 (ESRI, 2019) to identify SFDA by: (a) filling any sink with an area $< 3700 \text{ m}^2$ (i.e., 3^2 DEM cells); (b) burning lakes into the DEM; (c) fencing lakes that had no topographic lip at the outlet, and; (d) omitting stream segmentation. Sinks $\geq 3^2$ DEM cells, and associated basins, were thereby excluded from the delineation of each drainage basin, thereby allowing us to estimate ‘sink-free’ drainage area. GDA was delineated using the same workflow, but after having filled all upstream sinks except the lake itself. Both SFDA and GDA basins were crosschecked with watercourses in the National Research Council of Canada’s Canadian topographic map reference product (CanVec 2016) at a resolution of 1:50,000 to identify potential mismatches between adjacent watersheds. The furthest downstream cell in each lake was used as the pour point for that basin (ESRI, 2013), unless the lake was endorheic (no surface outlet). Calculated using this method, SFDA can be used as a reliable and reproducible estimate of ‘effective drainage area’ (cf., Martin 1983).

2.4 Meteorological data

Precipitation estimates for each lake were gathered from a combination of remotely sensed and instrumental data. Specifically, winter precipitation was extracted from the US National Weather Service's National Operational Hydrologic Remote Sensing Center SNOw Data Assimilation System (SNODAS, <https://nsidc.org/data/g02158>). For each lake, the total snow water equivalent (SWE; m³) was determined from both the GDA and SFDA of each lake prior to the commencement of the spring melt (15 April 2013). Liquid precipitation was summed from 16 April 2013 to 31 October 2013 from ECCC monitoring data and was interpolated using inverse distance-weighting to determine the local precipitation for each drainage basin.

2.5 Evaporation calculations

Application of the IMB approach to estimate hydrological parameters required additional information for each basin, including flux-weighted temperature and relative humidity. For all IMB formulations, temperature and relative humidity from the nearest ECCC gauging station were flux-weighted by evaporation to emphasize the importance of the ice-free season (Gibson et al. 2002a, 2005). Evaporation (e; mm) was calculated using the Meyer's Method which requires wind speed, temperature, and dew point temperature (Martin, 2002) as:

$$e = C \cdot K (V_w - V_a) \cdot (1 + 6.2139 \times 10^{-2} W) \cdot (1 + 3.28084 \times 10^{-5} \cdot A). \quad (1)$$

Here C is a coefficient of 10.1 because our analysis used observations of dew-point temperature (Martin, 2002), K is the metric conversion factor (0.750062), V_w is the saturated vapour pressure (mbar), V_a is the actual monthly mean vapour pressure (mbar), W is the monthly mean wind speed at 7.6 m above ground (km hour⁻¹), and A is the elevation above sea level of the climate station (m). Water temperature for estimation of V_w was calculated from air temperature at each lake using month-specific regression relationships for study area (Martin, 2002). As Meyer's

method for estimation of gross evaporation is most appropriate for small to moderate-sized lakes characteristic of this survey (Table 1 in Plancq et al., 2018), evaporation was not adjusted for variation in lake size (Martin, 2002) and we assume estimates of evaporation are well suited for evaluation of spatial gradients among lakes.

2.6 Water Isotope Analysis

Surface water samples were collected from all study lakes over the deepest point during 29 July to 31 August 2013. Lakes were sampled in clusters using two-day excursions. Water samples were filtered through a cellulose membrane filter (0.45- μm pore) and stored in airtight scintillation vials with conical-insert caps at 4 °C to prevent sample evaporation before analysis. Samples were analyzed for $\delta^2\text{H}$ and $\delta^{18}\text{O}$ using a Thermo Finnigan DeltaPlusXL isotope ratio mass spectrometer (IRMS) at the Institute of Environmental Change and Society, University of Regina, Canada. Isotopic values were normalized using a high and low secondary standard system that had been calibrated using international standards of Vienna Standard Mean Ocean Water 2 (VSMOW2) and Standard Light Antarctic Precipitation 2 (SLAP2). All isotope results are reported in δ notation in per mil units (‰) with measurement precision of 0.2 ‰ for $\delta^{18}\text{O}$ and 1.2 ‰ for $\delta^2\text{H}$. At each site, deuterium excess ($d\text{-excess} = \delta^2\text{H} - 8\delta^{18}\text{O}$) was calculated as an indicator of the magnitude of surface evaporation (Dansgaard, 1964; Gat, 2001).

Lake water isotope values (δ_L) were compared to the local meteoric water line (LMWL, $\delta^2\text{H} = 7.74 \delta^{18}\text{O} - 0.14$) derived from over a decade of data collected in Saskatoon Saskatchewan, (1990 – 2013), and calculated using the precipitation-amount-weighted least squares regression technique (Hughes and Crawford, 2012). Most inter-annual variability in the regional LMWL arises from variation in atmospheric teleconnections and major storm tracks (Birks and Edwards, 2009). To ensure that the LMWL from Saskatoon was comparable to other locations in southern

Saskatchewan, its isotope values were compared with those from other prairie locations, including a 3-year time series (2013-2016) of precipitation at Regina, Saskatchewan (230 km south), a LMWL from Calgary, Alberta (520 km west; Peng et al., 2004), and monthly mean precipitation values from Brandon, Manitoba (<https://waterisotopes.org>; 635 km southeast). Slopes of the four regional LMWL's varied from 7.44 to 7.73 with no distinct spatial pattern. Because this analysis revealed minimal differences among locations spanning our entire sampling area (Supplementary Fig. 1), slopes from the central Saskatoon LMWL were used for all survey calculations. To visualize the evolution of water isotopes due to evaporation (Gibson et al., 2016b), a lake-specific local evaporation line (LEL) was calculated for each basin using a linear regression of isotopic values from amount-weighted average precipitation (δ_p), the isotopic composition of lake waters in a closed-basin in which evaporation equals inflow (δ_{ss}), and the theoretical maximum (limiting) isotopic enrichment (δ^*).

2.7 Isotope mass balance theory

Isotope mass balances were estimated for each lake using a combination of local isotope determinations (lake water, δ_L local precipitation, δ_p), regional meteorological data (precipitation, temperature, evaporation, relative humidity), and basin characteristics (lake area, watershed area, lake volume), as outlined in Gibson et al. (2016a, b). Briefly, the following equations were used to describe a lake that is in hydrological and isotopic steady state and where there are negligible changes in annual water storage (lake level):

$$I = Q + E \quad (m^3) \quad (2)$$

$$I \delta_I = Q \delta_Q + E \delta_E \quad (\text{‰} m^3). \quad (3)$$

278 Here I , Q , and E are the volume of lake inflow, outflow, and evaporation (m^3) and their
279 associated isotope ratios (δ_I , δ_Q , and δ_E) in ‰ units. We assumed isotopic values of outflow were
280 the same as those of lake water ($\delta_Q \approx \delta_L$). Although changes in lake level occur in all systems due
281 to the spring freshet and subsequent summer evaporation, relatively little is known of the
282 magnitude of lake volume changes at most sites (cf. Pham et al. 2009), therefore it is impractical
283 to develop non-steady state models (Gibson, 2002).

284 In these calculations, groundwater was aggregated with surface transport within the inflow
285 term (I) because subterranean contributions are expected to be minor (Prepas and Shaw, 1990;
286 van der Kamp et al., 2008), unlike small prairie wetlands (Bam and Ireson, 2019), and direct
287 measurement of groundwater flux was not possible for most sites. Regardless, shallow
288 groundwater is predominately composed of local snowpack and cannot be distinguished from
289 meltwaters via stable isotope analyses alone (Jasechko et al., 2017). Moreover, given that
290 shallow groundwater recharge tends to be associated with snowmelt in spring, we assume that it
291 has not undergone evaporation.

292 Estimates of δ_I were based on the coupled isotope tracer method (CITM) of Yi et al. (2008)
293 that uses the δ_E and δ_L of each sample to create a sample-specific line and then approximates δ_I
294 from the intersection of the sample specific line and the LMWL. This method also assumes that
295 all lakes are headwater systems and that all inputs to the lake are unaffected by evaporation.
296 Uncertainty associated with using headwater models in lakes where inputs have previously been
297 subject to evaporation can overestimate evaporation by up to 30 % (Haig et al., 2020), therefore,
298 in this survey, models provide an upper limit to E/I for the 2013 hydrological year.

299 To quantify the water balance (E/I) of a headwater lake, equation 2 can be rearranged to
300 obtain the evaporation to inflow ratio (x):

$$x = \frac{E}{I} = \frac{(\delta_I - \delta_L)}{(\delta_E - \delta_L)}. \quad (4)$$

In the equation (4), lake water isotopic composition (δ_L) was measured, isotopic composition of inflow (δ_I) was modelled using CITM (Yi et al., 2008), while the isotopic composition of evaporated water vapour was modelled using the Craig & Gordon Model (Craig et al., 1965; Gibson & Edward 2002; Yi et al., 2008; Haig et al., 2020). Unlike many previous isotopic studies (e.g., Gibson & Edward 2002), the CITM couples $\delta^{18}\text{O}$ and $\delta^2\text{H}$ within the mass balance model, therefore we do not differentiate $\delta^{18}\text{O}$ -derived E/I from $\delta^2\text{H}$ -derived E/I.

Total inflow into a lake (I ; m^3) can then be obtained using evaporation (e) calculated using the Meyers method (Martin, 2002) and lake surface area (L_A) as;

$$I = \frac{e L_A}{\chi}. \quad (5)$$

Lake inflow (I) calculated in this manner integrates both direct precipitation on the lake surface, as well as overland flow, channelized stream inflow, and shallow groundwater inputs. Ungauged (overland or unmeasured) influx from the catchment (U ; m^3) can be estimated by subtracting estimates of direct precipitation input to the lake (p) from total inflow as,

$$U = \frac{e L_A}{\chi} - p L_A. \quad (6)$$

In general, drainage basins within the NGP exhibit low topographic relief resulting in dynamic watershed areas (W_A) that vary with p and antecedent moisture conditions (Stichling and Blackwell, 1957). Under these conditions, water yield (WY ; mm year^{-1}), or depth-equivalent runoff, can be used to standardize U to watershed area, according to;

$$WY = \frac{U}{W_A} \times 1000. \quad (7)$$

This equation was originally formulated for headwater systems and can be considered a lower limit for non-headwater systems due to the potential influence of upstream evaporation (Gibson et al., 2018). Subsequently, WY can be estimated for either GDA or SFDA for each lake using Eq. 6.

To evaluate how watershed characteristics affect catchment water yield, we first standardized WY to the amount of precipitation received by the catchment to calculate a runoff coefficient (C). Here, C represents the fraction of precipitation that falls within the watershed area that becomes lake input, a parameter which is commonly used by water managers to predict how inflow will vary as a function of precipitation;

$$C = \frac{WY}{p}. \quad (8)$$

In particular, C is often used to evaluate the presence of non-linear relationships between liquid runoff and streamflow (Dumanski et al., 2015; Ehsanzadeh et al., 2012, 2016). By bracketing estimates of water yield for each catchment using calculations based on SFDA and GDA, we sought to obtain an upper (using SFDA) and lower (using GDA) limit to ‘actual’ export of precipitation from the catchment.

2.8 Statistical analysis

Generalized additive models using latitude and longitude as predictors were used to estimate the spatial relationship for each hydrological (E/I, $\delta^{18}\text{O}$, water yield, runoff coefficient), meteorological (precipitation, water deficit) and landscape parameters (soil characteristics, land cover) via penalized tensor-product smooths. GAM’s are preferred over linear interpolations (e.g., inverse distance weighting) as they can quantify non-linear relationships between

predictors and responses. Herein, family and link functions were chosen for each model individually, based on the observed variable distribution, including Gaussian (e.g. $\delta^{18}\text{O}$), gamma (runoff coefficient) and beta relationships (% area as cropland). Links were specified to ensure model predictions remained within expected bounds of the parameter distribution. All calculations were completed in R statistical environment using the *mgcv* package (Wood, 2011; Wood et al., 2016).

Principal components analysis (PCA) were used to explore potential relationships between landscape characteristics, and IMB-derived estimates of lake hydrology, including $\delta^{18}\text{O}$, water balance (E/I), water yield, runoff coefficient. Specifically, we looked for potential relationships between hydrological characteristics and factors that are known to affect the transmission of water to surface water features. These landscape variables included; crop cover (%), grasslands (%), urban cover (%), forest cover (%), sink area (m^2), shape of the catchment ('form factor' from Zăvoianu, 1985), saturated hydraulic conductivity (cm h^{-1}), average distance between streams (m), average distance of overland flow (m; Stichling and Blackwell, 1957), drainage density (m^{-1}), sink fill volume (m^3), winter precipitation (m), and summer precipitation (m). Most variables required \log_{10} transformation. Landcover data were obtained from Agriculture and Agri-Food Canada Annual Crop Inventory database (AAFC, 2013). All PCAs were completed in the *vegan* package of R (Oksanen et al., 2018).

3. Results

3.1 Lakewater isotopes

Mean ($\pm \sigma$) isotopic values of prairie precipitation varied from December minima for $\delta^2\text{H}$ ($193.9 \pm 30.0 \text{ ‰}$) and $\delta^{18}\text{O}$ ($-24.83 \pm 4.1 \text{ ‰}$) to June maxima for both $\delta^2\text{H}$ ($-96.1 \pm 18.4 \text{ ‰}$) and $\delta^{18}\text{O}$ ($12.7 \pm 2.0 \text{ ‰}$) (Supplementary Fig 1). Consequently, mean precipitation values for winter

snow (01 Nov – 31 March) were significantly depleted ($\delta^{18}\text{O}_{\text{snow}}$, $-22.3 \pm 4.0 \text{ ‰}$) relative to long-term (01 April – 31 Oct) estimates for rain ($-13.72 \pm 4.1 \text{ ‰}$).

Overall, δ_{L} values ranged from -134.0 to -64.0 ‰ ($\mu \pm \sigma = -90.1 \pm 12.1 \text{ ‰}$) for $\delta^2\text{H}$ and -16.7 to -4.2 ‰ ($\mu \pm \sigma = -9.2 \pm 2.0 \text{ ‰}$) for $\delta^{18}\text{O}$ (Fig. 2). Lakewater isotope values deviated from the LMWL as expected due to evaporative concentration. Lake-specific LELs determined using the coupled isotope tracer method (not shown) exhibited generally shallower slopes ($3.5 \pm 0.9 \text{ ‰}$) than that estimated (slope = 7.7 ‰) for the regional LEL model (Fig. 2a).

3.2 Isotope mass balances

There was no detectable difference (Welch's t -test $p = 0.64$) between mean ($\pm \sigma$) isotope values for lake inflow (δ_{I} ; $-13.5 \pm 2.0 \text{ ‰}$) and summer precipitation rainfall (δ_{rain} ; $-13.72 \pm 4.1 \text{ ‰}$) (Figs. 3, 4a). In contrast, mean δ_{I} values were substantially greater than those of winter precipitation ($\delta^{18}\text{O}_{\text{snow}}$; $-22.3 \pm 4.0 \text{ ‰}$) with relatively little overlap in range (Fig. 3). Categorization of lakes revealed that 49.5% of sites were rainfall-dominated and no lakes were categorized as snowfall-dominated during 2013. This finding provides a sharp contrast to a previous survey of this region 2004, at which time most lakes were considered snowmelt-dominated (Pham et al. 2009) despite similar mean levels of total precipitation in 2004 (386 mm) and 2013 (346 mm).

Overall, the water balance (E/I) of most lakes was below unity, ranging from 0.46 to 0.71, with a mean ($\pm \sigma$) of 0.32 ± 0.16 (Fig. 4b). The distribution of E/I values among Saskatchewan prairie lakes was approximately normal, with a slight positive skew (Fig. 4b). Water yield and runoff coefficient both displayed strongly and positively skewed distributions with mean ($\pm \sigma$) values of $100.8 \pm 181.0 \text{ mm yr}^{-1}$ ($\bar{x} = 35.5 \text{ mm yr}^{-1}$), and $22.1 \pm 45.9 \text{ ‰}$ ($\bar{x} = 6.9 \text{ ‰}$), respectively, when calculated using GDA (Fig. 4c, d). These mean values increased approximately three-fold

to $311.9 \pm 367.4 \text{ mm yr}^{-1}$ ($\bar{x} = 201.1 \text{ mm yr}^{-1}$), and $68.9 \pm 89.0 \%$ ($\bar{x} = 41.1 \text{ mm yr}^{-1}$), respectively, when calculated using the smaller SFDA (Fig. 4e, f). Extreme values of the runoff coefficient greater than 100 % were found in four lakes when calculated using GDA and 18 lakes using the SFDA, indicating that these basins may receive inflows in excess of the volume of precipitation received within their catchment during the 2013 hydrological year.

3.3 Spatial patterns of isotopic-inferred hydrology

Meteorological data for the study year (2013) displayed a transverse pattern of precipitation deficit within the study area, from drier in south-west to wetter in the north-east (Supplementary Fig. 2). GAMs revealed that this pattern exhibited high spatial structure (deviance explained = 95.4 %; Table 2) and reflected heightened evaporation (Supplementary Fig. 2d) and relatively low winter precipitation (Supplementary Fig. 2a) in the southwest study region. In contrast, the magnitude of rainfall was similar across the entire study area ($\mu = 266.3$, $\sigma = 35.1 \text{ mm}$; Supplementary Fig 2b).

Spatial patterns of isotopically-derived lake hydrology metrics (δ_i , E/I, runoff, water yield, and runoff coefficient) were distinct and inconsistent with observed patterns in meteorological data from 2013 (Fig. 5; Supplementary Figs. 2, 3). Instead, IMBs revealed statistically significant patterns in many lake hydrology parameters including a marked west-to-east gradient of δ_i enrichment (Fig. 5a), a northwest-to-southeast decline in E/I (Fig. 5b), and a northwest-to-southeast increase in water yield (Fig. 5e) and runoff coefficient (Fig. 5f) when calculated using SFDA but not with GDA. GAM analyses revealed that spatial patterns were significant and substantial (26.6 – 43.8 % of deviance explained) for all isotope-derived parameters deviance (Table 2), although model fit was lower than those of the main climatic parameters (Supplementary Fig. 2).

3.4 Predictors of hydrological variability

Principal component analysis explained 19.4 % of variation among lake and landscape parameters the first axis (PC1) and 17.6 % on the second axis (PC2) when analyzed on the basis of GDA (Fig. 6, Supplementary Fig. 3). Here PC1 was correlated positively to E/I, grassland cover, soil sandiness, and hydraulic conductivity, and negatively to drainage density, lake area, sink volume, crop cover, evaporative stress (d-excess) and, to a lesser extent, maximum depth and distance between streams. In contrast, PC2 was correlated positively to water yield, runoff coefficient, drainage basin ratio, form factor, and forest cover, whereas few factors loaded strongly and negatively on PC2 (% grassland, sink volume). PC3 also explained 10.6 % of variance, and was correlated positively to winter precipitation and negatively to evaporation and drainage density (not shown). PCA analysis based on SFDA (Supplementary Fig. 4) yielded similar patterns (PC1 21.3 %, PC2 14.3 %, PC3 12.4 %) to those based on the GDA, with E/I loading positively on PC1, and runoff coefficient and water yield mainly loading positively on PC2. Spatial patterns of drainage density, soil sand content, and land-use cover (% grass, % cropland) are presented in Supplementary Fig. 5.

4. Discussion

Analysis of IMBs from 105 ungauged prairie lakes showed that hydrological processes in prairie lakes were strongly influenced by the supply of rainwater (Figs. 2c, 3) during years following pluvial episodes (Ahmari et al. 2015; Blais et al., 2015; Haig et al., 2020). This finding contrasts with previous reports showing that snowmelt controls water balance after multi-year droughts (Coles et al., 2017; Fang et al., 2007; Pham et al., 2009; Pomeroy et al., 2007; Shook and Pomeroy, 2012). Maps of isotope-derived hydrological parameters supported previous studies (Bemrose et al., 2009; Martin, 2002) by showing that evaporative forcing (as

E/I) was greatest in the northwestern portion of the study region (Fig. 5b), even though potential evaporation (Supplementary Fig. 2d) and precipitation deficit (Supplementary Fig. 2e) were greatest in the southwest during 2013. Multivariate analysis showed that regions with high E/I were characterized by soils with relatively high sand content and hydraulic conductivity (Fig. 6), suggesting an important role for infiltration of precipitation prior to transmission to lakes (van der Kamp 2001), such as seen in small wetlands with limited surface inflow (Bam and Ireson, 2019; van der Kamp and Hayashi 2009). Similarly, isotope-derived estimates of runoff coefficients and water yield co-varied with geophysical characteristics of the catchments (form factor, drainage basin ratio) and land use (% forest cover) in this sub-humid region. Although further validation is needed using well-instrumented catchments (Haig et al., 2020), this spatial survey suggests that application of IMBs across landscapes can provide managers with a new tool to better forecast how precipitation events are transformed into runoff, surface inflow, and the potential for flooding during extreme events (SWSA, 2012; Stadnyk et al., 2016).

4.1 Isotopic characterization of surface water hydrology

Using the coupled isotope tracer method (Yi et al., 2008), input waters were categorized as a mixture of summer and winter precipitation in 50.5 % of lakes, while the remaining 49.5 % were affected mainly by rainfall (Fig. 2). These results differ substantially from earlier IMB results which concluded that 72 % of lakes in this region were dominated by snowpack runoff following a two-year drought in 2004 (Pham et al., 2009). However, Pham et al. (2009) did not determine basin-specific δ_i as done herein, but instead used the methods of Gibson et al., (1993) in which the entire study area is modelled as if it had a common water source. Although lakes in the 2004 survey were found to be less snowfall-dominated when re-analyzed using the present basin-

specific method, winter precipitation remained an important contributor to lakewater isotope values in the 2004 survey (re-analysis not shown).

In the present study, the importance of rainwater was far greater than that assumed when river gauges alone are used to measure inflow, where > 80 % of inflow is estimated to occur during spring snowmelt rather than in summer (Fang et al., 2007; Shook and Pomeroy, 2012). Differences between earlier (Fang et al., 2007, Pham et al., 2009; Shook and Pomeroy, 2012) and present research may reflect the known increase in the importance of rainfall to lotic flow, from 7 % in 1975-1994 to 34 % during 2010-2014 (Dumanski et al., 2015). Given that annual meteorological conditions were similar in 2004 and 2013 (Supplementary Fig. 6), we infer that lake water balances depend strongly on antecedent conditions, with higher reliance on snowmelt following more arid intervals (Hanesiak et al., 2011; Starks et al., 2014) and a predominant effect of rainfall after more humid periods (Brimelow et al., 2014; Wheeler and Gober, 2013).

Low isotopic estimates of E/I (Figs. 2b, 4b) indicated that prairie lakes captured precipitation from their drainage basins even when the basins lacked obvious overland inflow. This finding contrasts the classical view of prairie lakes as “hydrologically-closed” endorheic basins (Hammer, 1986; LaBaugh et al., 1998; Last and Ginn, 2005; Pham et al., 2008; Winter and Change, 1998). These different perspectives may reflect the fact that IMBs can detect transient connections between hydrologic features that are difficult to capture based on geomorphic or flow features (Brooks et al., 2018). It is of interest that lakes remained highly reliant on inflow despite water samples being taken during the late summer to maximize the E/I values (Haig, 2019; Haig et al., 2020). Overall, E/I values in this survey ($\mu = 0.32$) were lower than those determined in a previous spatial survey ($\mu = 0.44$) by Pham et al. (2009), but were similar to contemporaneous values found elsewhere within the NGP (Brooks et al., 2014).

This study provided the first isotope-based estimates of water yield and runoff coefficients for lakes of the Canadian Prairies. Comparison of these parameters estimated from GDA and SFDA calculations (Figs. 4, 5; Supplementary Fig. 3) illustrates the importance of small-scale topographic variation in regulating surface runoff in regions of low topographic relief, as both parameters were greater when local sinks were not included in determinations. As first discussed by Stichling and Blackwell (1957), estimates of the contributing area for prairie lakes often shift in response to changes over diverse timescales from hours (storms), through seasons (air mass changes), and decades (climate systems) (Martin et al., 1983; PFRA, 2007; Stichling and Blackwell, 1957). In general, SFDA-derived values for water yield and runoff coefficient (Fig. 4e, f) were higher than those estimated previously from instrumental river data for Canadian Prairies (runoff coefficient 0.24 -22 %) (Dumanski et al., 2015; Ehsanzadeh et al., 2016), possibly reflecting the ‘fill-and-spill’ nature of small regional wetlands (Coles and McDonnell, 2018; Hayashi and van der Kamp, 2009; Spence and Woo, 2003). Further research will be required to identify the precise mechanisms underlying this pattern and to better understand potential non-linear relationships between meteorological forcing and landscape geomorphology as controls of runoff and contributing area.

Mean ($\pm\sigma$) water yield estimates calculated using the IMB approach using either GDA (100.7 ± 181.0 mm yr⁻¹) or SFDA (311.9 ± 367.4 mm yr⁻¹) greatly exceeded published values (20-50 mm yr⁻¹) for this region based on long-term stream flow records (Bemrose et al., 2009). However, water yield values were highly skewed (Fig. 4) and median values of 35.5 mm yr⁻¹ calculated using the GDA were within the range previously recorded (Bemrose et al., 2009). Some of this difference may reflect the fact that Bemrose’s (2009) calculations were made using estimates of effective drainage area derived from the PFRA using a difficult-to-replicate

approach based in part on expert opinion. In addition, the PFRA estimates of drainage basin area are calculated as “drainage basin which might be expected to entirely contribute runoff to the main stream during a flood with a return period of two years” (Martin et al., 1983), rather than the annual estimate used herein.

Other direct comparisons of lake- and stream-based approaches also produce contrasting estimates of catchment water yield. For example, comparison of lentic stable isotopes and stream instrumentation in adjacent northeastern Alberta demonstrate that lake-derived yields are often lower than lotic values (Bennett et al., 2008). In contrast, isotopic estimates of water yield from lakes in costal British Columbia, Canada, were greater than those derived from 30-year average conditions for regional rivers (Bemrose et al., 2009; Gibson et al., 2018). Finally, comparison of both measured and isotopic estimates of water yield based on decade-long analyses revealed strong correlations in both boreal (Gibson et al., 2018) and prairie environments (Haig et al., 2020). Taken together, these results suggest that variable relationships between instrumental and isotopic estimates of water yield may result from regional differences in geomorphic controls of runoff (e.g., soil permeability, hydrological conductivity) such as seen here (Figs. 6, Supplementary Fig. 4) or differences in the degree to which streams and lakes integrate hydro-climate signals.

Estimates of runoff coefficient based on IMBs of individual lakes were similar to previous calculations based on Water Survey of Canada (WSC) monitoring. In general, median values for GDA and SFDA bracket the runoff coefficients expected for this region, with GDA-based analyses suggesting strongly that little precipitation ($\mu = 22.1$ $\sigma = 45.9$, $\bar{x} = 6.9$ %) enters prairie lakes. However, given that this conclusion is sensitive to assumptions concerning the role of sinks within the catchments (e.g., SFDA $\mu = 68.9$, $\sigma = 89.0$, $\bar{x} = 41.1$ %), further research is

required to better resolve this issue. Previously, runoff coefficients have been derived solely from instrumented streams and not lakes (Dumanski et al., 2015; Ehsanzadeh et al., 2016) and are calculated to gain a more mechanistic understanding of how precipitation is transformed to channelized surface flow (Blume et al., 2007). Runoff coefficients measured in local streams are known to vary widely (0.24 - 22.0 %), with the high variability among studies attributed to differences in regional climate and land-use characteristics within study catchments (Dumanski et al., 2015; Ehsanzadeh et al., 2016). Given the importance of rainfall inferred from analysis of δ_l in this region (Figs. 2b, 3), and the elevated isotopically-derived estimates of runoff coefficient (above), we infer that summer precipitation may contribute more substantially to water balance of 'hydrologically-closed' prairie was previously assumed (Shook and Pomeroy, 2012), at least during some decades.

Runoff coefficients exceeding 100 % were rare in calculations using both GDA (4 % of lakes) and SFDA (17 %) (Fig. 4). In principle, such extreme values could indicate the presence of water inputs unrelated to precipitation and runoff (e.g., springs) during that hydrological year. For example, the highest runoff coefficient (380%) was identified for Harris Lake, a well-studied site known to be strongly influenced by groundwater (Last and Sauchyn, 1993). Similarly, high values were returned for Ressor Lake (207 %), a basin which receives water from a nearby management diversion (Mitchell and Prepas, 1990). Given that groundwater is thought to be a relatively small portion of water balance to most prairie lakes (Prepas and Shaw, 1990; van der Kamp et al., 2008), the very high runoff coefficients derived from calculations based on SFDA are not expected to be reliable during pluvial periods, when sinks are full and catchment storage is low. Instead, runoff coefficients above 100 % calculated using GDA may provide important

insights about the presence of subterranean inflows, or undocumented catchment modifications (farm drainages).

4.2 Meteorological and catchment predictors of isotope-derived lake hydrology

A low degree of spatial coherence between annual meteorology (Supplementary Fig. 2) and isotopically-measured water balance (E/I) patterns (Fig. 5) demonstrates that spatially-structured factors other than precipitation and evaporation may affect the hydrological balance of prairie lakes, even though E/I was correlated negatively to summer precipitation, as expected. As all survey lakes experienced a negative precipitation balance, we anticipated that they should also experience pronounced evaporative concentration during the ice-free period (Pham et al., 2009). Unexpectedly, lakes that experienced the largest meteorological water deficit also had some of the lowest E/I values, suggesting inflow not associated with direct precipitation was required to sustain lake levels (Fig. 5; Supplementary Fig. 2).

Variation between spatial pattern of lake hydrology and potential meteorological forcing mechanisms appeared to be related, in part, to local differences in soil permeability, land cover, and hydraulic conductivity (Fig. 6). Here we found that E/I values were elevated in northwestern sites where soils were sandy and drainage density in the catchment was low (Supplementary Fig. 5) suggesting high infiltration potential of soils. Based on the relatively low $\delta_i^{18}\text{O}$ values in the northwest region, we also infer that overland flow to lakes in this region may occur during spring melt when soils are frozen and infiltration is reduced (Pomeroy et al., 2007). In contrast, lakes in south-western catchments exhibited greater drainage capacity and would be expected to be more closely linked to meteorological controls. Regardless, the observation that spatial patterns of both E/I and δ_i recorded here were consistent with those documented nine years earlier by Pham et al (2009) suggests that the main control processes may be similar at the scale of decades.

The importance of local geomorphology, land use practices, and vegetation cover in controlling the water balance of lakes has been well documented by IMB for boreal lakes (Gibson et al., 2015), tundra environments (Balasubramaniam et al., 2015; Turner et al., 2014), and sub-continent studies in many ecozones (Brooks et al., 2014), but is less known in agricultural regions (but see wetlands research; van der Kamp et al., 1999, 2003). Factors such as basin elevation (Gibson et al., 2018), distance to river (Remmer et al., 2018), and bedrock characteristics (Arnoux et al., 2017a, b; Gibson et al., 2016) are known to be important local drivers in other lake regions. As expected, our PCA and correlation analyses showed that areas with high water stress were covered predominantly with crops (Fig. 6). Further, given that conversion of cropland to grass cover is known to cause desiccation of previously well-established wetlands (van der Kamp et al., 1999), it seems likely that human management of vegetation plays a strong role in regulating water runoff in the prairie region.

Differences in spatial patterns and absolute values of water yield and runoff coefficient calculated using SFDA and GDA points to the need for high resolution studies of lake hydrology in regions with low topographic relief such as the NGP. Challenges in quantifying the actual contributing area of catchments remain a critical uncertainty in models attempting to link meteorological phenomenon, lake hydrology, and the sustainability of surface water resources during a changing climate regime (Shook et al., 2015, 2013). For example, the general agreement between median values of water yield using the GDA calculation and estimates derived from regional monitoring programs supports the early statement by Stichling and Blackwell (1957) most of the GDA contributes to lake inflow during pluvial periods. In contrast, the apparent overestimation of hydrological parameters based on SFDA calculations suggests that the storage capacity of many depressions was limited during our survey and, therefore, the watershed was

represented better by the larger GDA. The presence of ‘full sinks’ may also explain the lack of relationships between the volume of sinks and various hydrological parameters. Finally, the negative association between sink volume and E/I values (Fig. 7) supports the suggestion that lakes within drainage basins with abundant sinks may have lower E/I values because of high connectivity between depressions and lakes (Brooks et al., 2018, MacKinnon et al., 2018), consistent with the ‘fill and spill’ model for regional wetlands (Coles and McDonnell, 2018).

5. Conclusions

Application of IMB techniques to prairie lakes provided an important means to study the effects of meteorological conditions, instrumented and ungauged inflow, and land characteristics in determining spatial patterns in lake hydrology. By better understanding the relative importance of precipitation originating as rain and snow, we explicitly address a scientific shortcoming in predicting how lakes of the NGP may respond to future climate change (Shook et al., 2015). In particular, this first prairie estimation of isotope-derived runoff coefficients integrates multiple processes that regulate moisture balance but which are difficult to quantify at large spatial scales. Clearly, further studies are needed in well-instrumented systems where runoff coefficient can be measured and compared over an extended time period to quantify how well isotopic determinations can capture changes in runoff coefficient associated with hydrological extremes, changes in land use, and manipulative alterations in surface drainage (Khaliq et al., 2018; van der Kamp et al. 1999).

The lack of consistency between spatial patterns of meteorological variables and isotope-derived lake hydrology allowed inferences about the relative role of land use processes and cryptic fluxes (e.g., groundwater) in regulating the water balance of lakes. Results suggest that physical characteristics in the surrounding catchment (e.g., sand content, drainage density), and

land use variables (e.g., cropland, grassland) may have important effects on the sustainability of prairie water bodies. Further studies are needed to test these associations and produce predictive models that allow managers to develop a spatially-diverse portfolio of plans to ensure sustainability of surface waters in the NGPs.

Declaration of Competing Interests

The authors declare that they have no known competing financial interests or personal relationships that could have appeared to influence the work reported in this paper.

Acknowledgements

We thank all members of the Limnology Laboratory involved in sample collection and analysis, including E. Hillis, J. Wolfe, and C. Morell. This work was supported by the NSERC Canada post-graduate awards, NSERC Discovery Grants, Canada Research Chairs, Canada Foundation for Innovation, Province of Saskatchewan, University of Regina, and Queen's University Belfast. We acknowledge that the study lakes are located within Treaty 2, 4, 5, and 6 territories, the homelands of the Cree, Saulteaux, Lakota, Dakota, Natoka and Metis peoples. We acknowledge the willingness of the First Nations of Saskatchewan to share and protect these water resources. This is a contribution of the Qu'Appelle Valley long-term ecological research program (QU-LTER).

Author Contribution Statement

HAH and PRL designed the study, HAH, NMH, YY, KH, and PRL designed the analysis, BW and HAH conducted all isotope analyses, HAH and GLS calculated isotope mass balances, KH and HAH developed and undertook the drainage basin analysis, HAH lead the writing of the

manuscript, all authors commented on and revised the manuscript, all author approved the final versions, and PRL coordinated and funded the data collections.

Appendix A. Supplementary Data

Supplementary data to this article can be found online at
<https://doi.org/10.116/j.hydroa.XXXX.xxxxxxxx>

References

- Agriculture and Agri-Food Canada. 2013. Annual Crop Inventory. Ottawa, Ontario, Canada.
<https://open.canada.ca/data/en/dataset/ba2645d5-4458-414d-b196-6303ac06c1c9>
- Ahmari, H., Blais, E.-L., Greshuk, J., 2015. The 2014 flood event in the Assiniboine River Basin: Causes, assessment and damage. *Can. Water Resour. J.* 41, 85–93.
<https://doi.org/10.1080/07011784.2015.1070695>
- Akinremi, O., McGinn, S., Cutforth, H., 1999. Precipitation trends on the Canadian Prairies. *J. Climate* 12, 2996–3003. [https://doi.org/10.1175/1520-0442\(1999\)012<2996:PTOTCP>2.0.CO;2](https://doi.org/10.1175/1520-0442(1999)012<2996:PTOTCP>2.0.CO;2)
- Arnoux, M., Barbecot, F., Gibert-Brunet, E., Gibson, J.J., Rosa, E., Noret, A., Monvoisin, G., 2017a. Geochemical and isotopic mass balances of kettle lakes in southern Quebec (Canada) as tools to document variations in groundwater quantity and quality. *Env. Earth Sci.* 76, 106.
<https://doi.org/10.1007/s12665-017-6410-6>
- Arnoux, M., Gibert-Brunet, E., Barbecot, F., Guillon, S., Gibson, J.J., Noret, A., 2017b. Interactions between groundwater and seasonally ice-covered lakes: Using water stable isotopes and radon-222 multilayer mass balance models. *Hydrol. Process.* 31, 2566–2581.
<https://doi.org/10.1002/hyp.11206>
- Asong, Z.E., Khaliq, M.N., Wheeler, H.S., 2016. Projected changes in precipitation and temperature over the Canadian Prairie Provinces using the Generalized Linear Model statistical downscaling approach. *J. Hydrol.* 539, 429–446.
<https://doi.org/10.1016/j.jhydrol.2016.05.044>
- Balasubramaniam, A., Hall, R.I., Wolfe, B.B., Sweetman, J.N., Wang, X., 2015. Source water inputs and catchment characteristics regulate limnological conditions of shallow subarctic lakes (Old Crow Flats, Yukon, Canada). *Can. J. Fish. Aquat. Sci.* 72, 1058–1072.
<https://doi.org/10.1139/cjfas-2014-0340>

676 Bam, E.K.P., Ireson, A.M., 2019. Quantifying the wetland water balance: A new isotope-based
677 approach that includes precipitation and infiltration. *J. Hydrol.* 570, 185-200. [https://doi.org/](https://doi.org/10.1016/j.jhydrol.2018.12.032)
678 [10.1016/j.jhydrol.2018.12.032](https://doi.org/10.1016/j.jhydrol.2018.12.032)

679

680 Bemrose, R., Kemp, L., Henry, M., Soulard, F. 2009. The Water Yield for Canada As a Thirty-
681 year Average (1971 to 2000): Concepts, Methodology and Initial Results (No. 7).
682 Statistics Canada, Ottawa, ON, Canada.

683

684 Bennett, K.E., Gibson, J.J., McEachern, P.M., 2008. Water-yield estimates for critical loadings
685 assessment: Comparisons of gauging methods versus an isotopic approach. *Can. J. Fish.*
686 *Aquat. Sci.* 65, 83–99. <https://doi.org/10.1139/f07-155>

688 Birks, J.S., Edwards, T.W., 2009. Atmospheric circulation controls on precipitation isotope-
689 climate relations in western Canada. *Tellus B* 61, 566–576. [https://doi.org/10.1111/j.1600-](https://doi.org/10.1111/j.1600-0889.2009.00423.x)
690 [0889.2009.00423.x](https://doi.org/10.1111/j.1600-0889.2009.00423.x)

691

692 Blais, E.-L., Greshuk, J., Stadnyk, T., 2015. The 2011 flood event in the Assiniboine River
693 Basin: Causes, assessment and damages. *Can. Water Resour. J.* 41, 74–84.
694 <https://doi.org/10.1080/07011784.2015.1046139>

695

696 Blume, T., Zehe, E., Bronstert, A., 2007. Rainfall—runoff response, event-based runoff
697 coefficients and hydrograph separation. *Hydrol. Sci. J.* 52, 843–862. [https://doi.org/10.1623/](https://doi.org/10.1623/hysj.52.5.843)
698 [hysj.52.5.843](https://doi.org/10.1623/hysj.52.5.843)

699

700 Bonsal, B., Shabbar, A., 2008. Impacts of large-scale circulation variability on low streamflows
701 over Canada: A review. *Can. Water Resour. J.* 33, 137–154.
702 <https://doi.org/10.4296/cwrj3302137>

704 Bonsal, B.R., Cuell, C., Wheaton, E., Sauchyn, D.J., Barrow, E., 2017. An assessment of
705 historical and projected future hydro-climatic variability and extremes over southern
706 watersheds in the Canadian Prairies. *Int. J. Climatol.* 37, 3934–3948. [https://doi.org/10.1002/](https://doi.org/10.1002/joc.4967)
707 [joc.4967](https://doi.org/10.1002/joc.4967)

709 Brimelow, J., Stewart, R., Hanesiak, J., Kochtubajda, B., Szeto, K., Bonsal, B., 2014.
710 Characterization and assessment of the devastating natural hazards across the Canadian
711 Prairie Provinces from 2009 to 2011. *Nat. Hazard.* 73, 761–785.
712 <https://doi.org/10.1007/s11069-014-1107-6>

714 Brooks, J.R., Gibson, J.J., Birks, S.J., Weber, M.H., 2014. Stable isotope estimates of
715 evaporation: Inflow and water residence time for lakes across the United States as a tool for
716 national lake water quality assessments. *Limnol. Oceanogr.* 59, 2150–2165.
717 <https://doi.org/10.4319/lo.2014.59.6.2150>

718

719 Brooks, J.R., Mushet, D.M., Vanderhoof, M.K., Leibowitz, S.G., Christensen, J.R., Neff, B.P.,
720 Rosenberry, D.O., Rugh, W.D., Alexander, L.C., 2018. Estimating Wetland Connectivity to

- Streams in the Prairie Pothole Region: An Isotopic and Remote Sensing Approach. *Water Resour. Res.* 54, 955-977. <https://doi.org/10.1002/2017WR021016>
- CanVec, 2016. Topographic Data of Canada - CanVec Series. National Research Council of Canada, Ottawa, Canada. <https://open.canada.ca/data/en/dataset/8ba2aa2a-7bb9-4448-b4d7-f164409fe056>
- Cole, A., 2013. AAFC Annual Unit Runoff in Canada. Agriculture and Agri-Food Canada. <https://open.canada.ca/data/en/dataset/a905bafc-74b5-4ec5-b5f9-94b2e19815d0>
- Coles, A., McConkey, B., McDonnell, J.J., 2017. Climate change impacts on hillslope runoff on the northern Great Plains, 1962-2013. *J. Hydrol.* 550, 538–548. <https://doi.org/10.1016/j.jhydrol.2017.05.023>
- Coles, A.E., McDonnell, J.J., 2018. Fill and spill drives runoff connectivity over frozen ground. *J. Hydrol.* 558, 115–128. <https://doi.org/10.1016/j.jhydrol.2018.01.016>
- Carey, S.K., Pomeroy, J.W., 2009. Progress in Canadian snow and frozen ground hydrology, 2003-2007. *Can. Water Resour. J.* 34, 127–138. <https://doi.org/10.4296/cwrj3402127>
- Craig, H., Gordon, L., Tongiorgi, E., 1965. Deuterium and oxygen 18 variations in the ocean and the marine atmosphere, in: *Stable Isotopes in Oceanographic Studies and Paleotemperatures*. Laboratorio di Geologia Nucleare, pp. 9–130.
- Dansgaard, W., 1964. Stable isotopes in precipitation. *Tellus* 4, 436-467. <https://doi.org/10.1111/j.2153-3490.1964.tb00181.x>
- Dibike, Y., Prowse, T., Bonsal, B., O’Neil, H., 2016. Implications of future climate on water availability in the western Canadian river basins. *Int. J. Climatol.* 37, 3247–3263. <https://doi.org/10.1002/joc.4912>
- Dumanski, S., Pomeroy J.W., Westbrook C.J. 2015. Hydrological regime changes in a Canadian Prairie basin. *Hydrol. Process.* 29, 3893-3904. <https://doi.org/10.1002/hyp.10567>
- Ehsanzadeh, E., Spence, C., van der Kamp, G., McConkey, B.G., 2012. On the behaviour of dynamic contributing areas and flood frequency curves in North American Prairie watersheds. *J. Hydrol.* 414, 364–373. <https://doi.org/10.1016/j.jhydrol.2011.11.007>
- Ehsanzadeh, E., van der Kamp, G., Spence, C., 2012. The impact of climatic variability and change in the hydroclimatology of Lake Winnipeg watershed. *Hydrol. Process.* 26, 2802–2813. <https://doi.org/10.1002/hyp.8327>
- Ehsanzadeh, E., van der Kamp, G., Spence, C., 2016. On the changes in long-term streamflow regimes in the North American Prairies. *Hydrol. Sci. J.* 61, 64–78. <https://doi.org/10.1080/02626667.2014.967249>

- ERSI, 2019. Arc Hydro: Overview of Terrain Preprocessing Workflows. ESRI California. 23 pp.
- Fang, X., Minke, A., Pomeroy, J.W., Brown, T., Westbrook, C.J., Guo, X., Guangul, S., 2007. A Review of Canadian Prairie Hydrology: Principles, Modelling and Response to Land Use and Drainage Change (No. 2), Center for Hydrology. University of Saskatchewan, Saskatoon, Canada.
- Fang, X., Pomeroy, J.W., Westbrook, C.J., Guo, X., Minke, A.G., Brown, T., 2010. Prediction of snowmelt derived streamflow in a wetland dominated prairie basin. Hydrol. Earth Sys. Sci. 14, 991–1006. <https://doi.org/10.5194/hess-14-991-2010>
- Fekete, B.M., Gibson, J.J., Aggarwal, P., Vörösmarty, C.J., 2006. Application of isotope tracers in continental scale hydrological modeling. J. Hydrol. 330, 444–456. <https://doi.org/10.1016/j.jhydrol.2006.04.029>
- Gan, T., Tanzeeba, S., 2012. Potential impact of climate change on the water availability of South Saskatchewan River Basin. Climate Change 112, 355–386. <https://doi.org/10.1007/s10584-011-0221-7>
- Gao, Z., Niu, F., Lin, Z., Luo, J., Yin, G., Wang, Y., 2018. Evaluation of thermokarst lake water balance in the Qinghai–Tibet Plateau via isotope tracers. Sci. Total Environ. 636, 1–11. <https://doi.org/10.1016/j.scitotenv.2018.04.103>
- Gat, J.R., 1995. Stable isotopes of fresh and saline lakes. Springer-Verlag, New York, pp. 139–165 in Lerman, A., Imboden, D.M., and Gat, J.R. [eds.], The Physics and Chemistry of Lakes. Springer, New York.
- Gat, J.R., 2001. Environmental Isotopes in the Hydrological Cycle, 39. International Atomic Energy Agency, Paris. International atomic energy agency and United Nations Educational, Scientific and Cultural Organization.
- Gibson, J.J., Edwards, T., W., D., Bursey, G.G., Prowse T.D. 1993. Estimating evaporation using stable isotopes: Quantitative results and sensitivity analysis for two catchments in northern Canada. Nord. Hydrol. 24, 79–94.
- Gibson, J.J., 2002. A new conceptual model for predicting isotopic enrichment of lakes in seasonal climates. Past Global Chang. 10, 10–11. <https://doi.org/10.22498/pages.10.2.10>
- Gibson, J.J., Edwards, T.W., 2002. Regional water balance trends and evaporation-transpiration partitioning from a stable isotope survey of lakes in northern Canada. Global Biogeochem. Cycles 16, 10-1-10–14. <https://doi.org/10.1029/2001GB001839>
- Gibson, J.J., Edwards, T.W., Birks, S., Amour, S.N., Buhay, W., McEachern, P., Wolfe, B., Peters, D., 2005. Progress in isotope tracer hydrology in Canada. Hydrol. Process. 19, 303–327. <https://doi.org/10.1002/hyp.5766>

813 Gibson, J.J., Reid, R., 2010. Stable isotope fingerprint of open-water evaporation losses and
814 effective drainage area fluctuations in a subarctic shield watershed. *J. Hydrol.* 381, 142–150.
815 <https://doi.org/10.1016/j.jhydrol.2009.11.036>

817 Gibson, J.J., Reid, R., 2014. Water balance along a chain of tundra lakes: A 20-year isotopic
818 perspective. *J. Hydrol.* 519, 2148–2164. <https://doi.org/10.1016/j.jhydrol.2014.10.011>
819

820 Gibson, J.J., Birks, S.J., Yi, Y., Vitt, D.H., 2015. Runoff to boreal lakes linked to land cover,
821 watershed morphology and permafrost thaw: A 9-year isotope mass balance assessment.
822 *Hydrol. Process.* 29, 3848–3861. <https://doi.org/10.1002/hyp.10502>
823

824 Gibson, J.J., Birks, S.J., Yi, Y., 2016a. Stable isotope mass balance of lakes: A contemporary
825 perspective. *Quat. Sci. Rev.* 131, 316–328. <https://doi.org/10.1016/j.quascirev.2015.04.013>

827 Gibson, J.J., Birks, S.J., Yi, Y., Moncur, M.C., McEachern, P.M., 2016b. Stable isotope mass
828 balance of fifty lakes in central Alberta: Assessing the role of water balance parameters in
829 determining trophic status and lake level. *J. Hydrol. Region. Stud.* 6, 13–25.
830 <https://doi.org/10.1016/j.ejrh.2016.01.034>

832 Gibson, J.J., Birks, S.J., Yi, Y., Shaw, P., Moncur, M.C., 2018. Isotopic and geochemical
833 surveys of lakes in coastal B.C.: Insights into regional water balance and water quality
834 controls. *J. Hydrol. Region. Stud.* 17, 47–63. <https://doi.org/10.1016/j.ejrh.2018.04.006>

836 Gibson, J.J., Birks, S.J., Moncur, M., 2019. Mapping water yield distribution across the South
837 Athabasca Oil Sands (SAOS) area: Baseline surveys applying isotope mass balance of lakes.
838 *J. Hydrol. Region. Stud.* 21, 1–13. <https://doi.org/10.1016/j.ejrh.2018.11.001>

840 Haig, H.A., 2019. Analysis of lakewater isotopes in the northern Great Plains: Insights from
841 long-term monitoring and spatial surveys. PhD Thesis. University of Regina, Regina,
842 Canada. 179 pp.
843

844 Haig, H.A., Hayes, N.M., Simpson, G.L., Wissel, B., Hodder, K.R., Leavitt, P.R., 2020.
845 Comparison of isotopic mass balance and instrumental techniques as estimates of basin
846 hydrology in seven connected lakes over 12 years. *J. Hydrol.* X 6, 100046.
847 <https://doi.org/10.1016/j.hydroa.2019.100046>
848

849 Hammer, U.T., 1986. Saline Lake Resources of the Canadian Prairies. *Can. Water Res. J.* 11,
850 43–57. <https://doi.org/10.4296/cwrj1101043>
851

852 Hanesiak, J., and others., 2011. Characterization and Summary of the 1999–2005 Canadian
853 Prairie Drought. *Atmosphere-Ocean* 49, 421–452.
854 <https://doi.org/10.1080/07055900.2011.626757>
855

856 Hayashi, M., van der, Kamp, G., 2009. Groundwater-wetland ecosystem interaction in the
857 semiarid glaciated plains of North America. *Hydrogeology Journal* 17, 203–214.
858 <https://doi.org/10.1007/s10040-008-0367-1>

859
860 Hayashi, M., van der Kamp, G., Rosenberry, D.O., 2016. Hydrology of prairie wetlands:
861 Understanding the integrated surface-water and groundwater processes. *Wetlands* 36, 237–
862 254. <https://doi.org/10.1007/s13157-016-0797-9>

864 Hughes, C., Crawford, J., 2012. A new precipitation-weighted method for determining the
865 meteoric water line for hydrological applications demonstrated using Australian and global
866 GNIP data. *J. Hydrol.* 464–465, 344–351. <https://doi.org/10.1016/j.jhydrol.2012.07.029>

867
868 Jacques, J.-M., Huang, Y.A., Zhao, Y., Lapp, S.L., Sauchyn, D.J., 2014. Detection and
869 attribution of variability and trends in streamflow records from the Canadian Prairie
870 Provinces. *Can. Water Res. J.* 39, 270–284. <https://doi.org/10.1080/07011784.2014.942575>

871
872 Jasechko, S., Perrone, D., Befus, K.M., Bayani Cardenas, M., Ferguson, G., Gleeson, T.,
873 Luijendijk, E., McDonnell, J.J., Taylor, R.G., Wada, Y., Kirchner, J.W., 2017. Global
874 aquifers dominated by fossil groundwaters but wells vulnerable to modern contamination.
875 *Nature Geosci.* 10, 425–429. <https://doi.org/10.1038/ngeo2943>

877 Khaliq, M., Sushama, L., Monette, A., Wheeler, H.S., 2015. Seasonal and extreme precipitation
878 characteristics for the watersheds of the Canadian Prairie Provinces as simulated by the
879 NARCCAP multi-RCM ensemble. *Climate Dynam.* 44, 255–277.
880 <https://doi.org/10.1007/s00382-014-2235-0>

882 LaBaugh, J.W., Winter, T.C., Rosenberry, D.O., Schuster, P.F., Reddy, M.M., Aiken, G.R.,
883 1997. Hydrological and chemical estimates of the water balance of a closed-basin lake in
884 north central Minnesota. *Water Resour. Res.* 33, 2799–2812.
885 <https://doi.org/10.1029/97WR02427>

886
887 LaBaugh, J.W., Winter, T.C., Rosenberry, D.O., 1998. Hydrologic functions of prairie wetlands.
888 *Great Plains Res.* 8, 17–37.

889
890 Last, W.M., Ginn, F.M., 2005. Saline systems of the Great Plains of western Canada: an
891 overview of the limnogeology and paleolimnology. *Saline Syst.* 1, 1–38.
892 <https://doi.org/10.1186/1746-1448-1-10>

893
894 Last, W. M., Sauchyn, D. J. 1993. Mineralogy and lithostratigraphy of Harris Lake,
895 southwestern Saskatchewan, Canada. *J. Paleolimnol.* 9, 23–39.
896 <https://doi.org/10.1007/BF00680033>

897
898 MacKinnon, B.D., Sagin, J., Baulch, H.M., Lindenschmidt, K.-E., Jardine, T.D., 2016. Influence
899 of hydrological connectivity on winter limnology in floodplain lakes of the Saskatchewan
900 River Delta, Saskatchewan. *Can. J. Fish. Aquat. Sci.* 73, 140–152.
901 <https://doi.org/10.1139/cjfas-2015-0210>

902
903 Mahmood, T.H., Pomeroy, J.W., Wheeler, H.S., Baulch, H.M., 2017. Hydrological responses to
904 climatic variability in a cold agricultural region. *Hydrol. Process.* 31, 854–870.

<https://doi.org/10.1002/hyp.11064>

- Masud, Khaliq, M., Wheeler, H.S., 2017. Projected changes to short- and long-duration precipitation extremes over the Canadian Prairie Provinces. *Climate Dynam.* 49, 1597–1616. <https://doi.org/10.1007/s00382-016-3404-0>
- Martin, F.R.J., Mowchenko, M., Meid, P.O., 1983. PFRA: The Determination of Gross and Effective Drainage Areas in the Prairie Province. Hydrology Report 104. Prairie Farm Rehabilitation Administration, Regina, Saskatchewan, Canada.
- Martin, F.R., 2002. Gross Evaporation for the 30-year Period 1971-2000 in the Canadian Prairies. Report 143. Prairie Farm Rehabilitation Administration, Regina, Saskatchewan, Canada.
- McCullough, G.K., Page, S.J., Hesslein, R.H., Stainton, M.P., Kling, H.J., Salki, A.G., Barber, D.G., 2012. Hydrological forcing of a recent trophic surge in Lake Winnipeg. *J. Great Lakes Res.* 38, 95–105. <https://doi.org/10.1016/j.jglr.2011.12.012>
- McNamara, J., Kane, D., Hinzman, L., 1998. An analysis of streamflow hydrology in the Kuparuk River Basin, Arctic Alaska: a nested watershed approach. *J. Hydrol.* 206, 39–57. [https://doi.org/10.1016/S0022-1694\(98\)00083-3](https://doi.org/10.1016/S0022-1694(98)00083-3)
- Michels, A., Laird, K.R., Wilson, S.E., Thomson, D., Leavitt, P.R., Oglesby, R.J., Cumming, B.F., 2007. Multidecadal to millennial-scale shifts in drought conditions on the Canadian prairies over the past six millennia: implications for future drought assessment. *Global Change Biol.* 13, 1295–1307. <https://doi.org/10.1111/j.1365-2486.2007.01367.x>
- Mitchell, P., Prepas, E., 1990. Atlas of Alberta lakes. University of Alberta Press, Edmonton, Canada. pp.
- Narancic, B., Wolfe, B.B., Pienitz, R., Meyer, H., Lamhonwah, D., 2017. Landscape-gradient assessment of thermokarst lake hydrology using water isotope tracers. *J. Hydrol.* 545, 327–338. <https://doi.org/10.1016/j.jhydrol.2016.11.028>
- Oksanen, J., Guillaume Blanchet, F., Friendly, M., Kindt, R., Legendre, P., McGlinn, D., Minchin, P.R., O'Hara, R.B., Simpson, G.L., Solymos, P., Stevens, M.H.H., Szoecs, E., Wagner, H., 2018. Vegan: Community Ecology Package. R package version 2.4-4. <https://cran.r-project.org/>
- Peng, H., Mayer, B., Harris, S., Krouse, R.H., 2004. A 10-yr record of stable isotope ratios of hydrogen and oxygen in precipitation at Calgary, Alberta, Canada. *Tellus B* 56, 147–159. <https://doi.org/10.3402/tellusb.v56i2.16410>
- PFRA, 2007. PFRA: Watershed Project. Prairie Farm Rehabilitation Administration. Government of Canada, Regina, Saskatchewan, Canada.

- Pham, S.V., Leavitt, P.R., McGowan, S., 2008. Spatial variability of climate and land-use effects on lakes of the northern Great Plains. *Limnol. Oceanogr.* 53, 728–742. <https://doi.org/10.4319/lo.2008.53.2.0728>
- Pham, S.V., Leavitt, P.R., McGowan, S., Wissel, B., Wassenaar, L.I., 2009. Spatial and temporal variability of prairie lake hydrology as revealed using stable isotopes of hydrogen and oxygen. *Limnol. Oceanogr.* 54, 101–118. <https://doi.org/10.4319/lo.2009.54.1.0101>
- Plancq, J., Cavazzin, B., Juggins, S., Haig, H.A., Leavitt, P.R., Toney, J.L., 2018. Assessing environmental controls on the distribution of long-chain alkenones in the Canadian Prairies. *Org. Geochem.* 117, 43–55. <https://doi.org/10.1016/j.orggeochem.2017.12.005>
- Pomeroy, J.W., Gray, D.R., Brown, T., Hedstrom, N.R., Quinton, W.L., Granger, R.J., Carey, S.K., 2007. The Cold Regions Hydrological Model: A platform for basing process representation and model structure on physical evidence. *Hydrol. Process.* 21, 2650–2667. <https://doi.org/10.1002/hyp.6787>
- Prepas, E.E., Shaw, R.D., 1990. Groundwater-lake interactions: II Nearshore seepage patterns and the contribution of ground water to lakes in central Alberta. *J. Hydrol.* 119, 121–136. [https://doi.org/10.1016/0022-1694\(90\)90038-Y](https://doi.org/10.1016/0022-1694(90)90038-Y)
- Remmer, C.R., Klemm, W.H., Wolfe, B.B., Hall, R.I., 2018. Inconsequential effects of flooding in 2014 on lakes in the Peace-Athabasca Delta (Canada) due to long-term drying. *Limnol. Oceanogr.* 63, 1502–1518. <https://doi.org/10.1002/lno.10787>
- Rodell, M., Famiglietti, J.S., Wiese, N.D., Reager, J.T., Beaudoing, H.K., Landerer, F.W., Lo, M.-H., 2018. Emerging trends in global freshwater availability. *Nature* 557, 651–659. <https://doi.org/10.1038/s41586-018-0123-1>
- Saskatchewan Water Security Agency, SWSA, 2012. 25 year Saskatchewan Water Security Plan. Saskatchewan Water Security Agency. Regina, Saskatchewan, Canada. 53 pp.
- Savenije, H., 1996. The runoff coefficient as the key to moisture recycling. *J. Hydrol.* 176, 219–225. [https://doi.org/10.1016/0022-1694\(95\)02776-9](https://doi.org/10.1016/0022-1694(95)02776-9)
- Shook, K., Pomeroy, J.W., 2010. Hydrological effects of the temporal variability of the multi-scaling of snowfall on the Canadian Prairies. *Hydrol. Earth Syst. Sci.* 14, 1195–1203. <https://doi.org/10.5194/hess-14-1195-2010>
- Shook, K., Pomeroy, J.W., 2012. Changes in the hydrological character of rainfall on the Canadian prairies. *Hydrol. Process.* 26, 1752–1766. <https://doi.org/10.1002/hyp.9383>
- Shook, K., Pomeroy, J.W., Spence, C., Boychuk, L., 2013. Storage dynamics simulations in prairie wetland hydrology models: Evaluation and parameterization. *Hydrol. Process.* 27, 1875–1889. <https://doi.org/10.1002/hyp.9867>

- 997 Shook, K., Pomeroy, J.W., van der Kamp, G., 2015. The transformation of frequency
 998 distributions of winter precipitation to spring streamflow probabilities in cold regions; case
 999 studies from the Canadian Prairies. J. Hydrol. 521, 395–409.
 1000 <https://doi.org/10.1016/j.jhydrol.2014.12.014>
- 1002 Spence, C., Woo, M., 2003. Hydrology of subarctic Canadian shield: Soil-filled valleys. J.
 1003 Hydrol. 279, 151–166. [https://doi.org/10.1016/S0022-1694\(03\)00175-6](https://doi.org/10.1016/S0022-1694(03)00175-6)
 1004
- 1005 Stadnyk, T., Dow, K., Waxney, L., Blais, E.-L., 2016. The 2011 flood event in the Red River
 1006 Basin: Causes, assessment and damages. Can. Water Resour. J. 41, 65–73.
 1007 <https://doi.org/10.1080/07011784.2015.1008048>
- 1009 Starks E., Cooper R., Leavitt P.R., Wissel B., 2014. Effects of drought and pluvial periods on fish
 1010 and zooplankton communities in prairie lakes: Systematic and asystematic responses.
 1011 Global Change Biol. 20, 1032–1042. <https://doi.org/10.1111/gcb.12359>
 1012
- 1013 Stichling, W., Blackwell, S.R., 1957. Drainage area as a hydrological factor on the glaciated
 1014 Canadian Prairies. IUGG Proc., 111, 365–376.
 1015
- 1016 Thornthwaite, C.W., 1948. An approach toward a rational classification of climate. Geogr. Rev.
 1017 38, 55–94. <https://doi.org/210739>
- 1019 Turner, K.W., Wolfe, B.B., Edwards, T.W., Lantz, T.C., Hall, R.I., Larocque, G., 2014. Controls
 1020 on water balance of shallow thermokarst lakes and their relations with catchment
 1021 characteristics: A multi-year, landscape-scale assessment based on water isotope tracers and
 1022 remote sensing in Old Crow Flats, Yukon (Canada). Global Change Biol. 20, 1585–1603.
 1023 <https://doi.org/10.1111/gcb.12465>
- 1025 van der Kamp, G., Stolte, W.J., Clark, R.G., 1999. Drying out of small prairie wetlands after
 1026 conversion of their catchments from cultivation to permanent brome grass. Hydrol. Sci. J.
 1027 44:387–397. <https://doi.org/10.1080/02626669909492234>
 1028
- 1029 van der Kamp G., 2001. Methods for determining the *in situ* hydraulic conductivity of shallow
 1030 aquitards-an overview. Hydrogeol. J. 9: 5–16. <https://doi.org/10.1007/s100400000118>
 1031
- 1032 van der Kamp, G., Hayashi, M., Gallén, D., 2003. Comparing the hydrology of grassed and
 1033 cultivated catchments in the semi-arid Canadian prairies. Hydrol. Process. 17: 559–575.
 1034 <https://doi.org/10.1002/hyp.1157>
 1035
- 1036 van der Kamp, G., Keir, D., Evans, M.S., 2008. Long-term water level changes in closed-basin
 1037 lakes of the Canadian Prairies. Can. Water Resour. J. 33, 23–38.
 1038 <https://doi.org/10.4296/cwrj3301023>
 1039
- 1040 van der Kamp, G., Hayashi, M., 2009. Groundwater-wetland ecosystem interaction in the
 1041 semiarid glaciated plains of North America. Hydrogeol. J. 17: 203–214.
 1042 <https://doi.org/10.1007/s10040-008-0367-1>

Vanderhoof, M.K., Alexander, L.C., Todd, J.M., 2016. Temporal and spatial patterns of wetland extent influence variability of surface water connectivity in the Prairie Pothole Region, United States. *Landsc. Ecol.* 31, 805–824. <https://doi.org/10.1007/s10980-015-0290-5>

Wheater, H.S., Gober, P., 2013. Water security in the Canadian Prairies: Science and management challenges. *Phil. Trans. R. Soc. A* 371, 20120409. <https://doi.org/10.1098/rsta.2012.0409>

Winter, T.C., Change, D.O., 1998. Hydrology of prairie pothole wetlands during drought and deluge: A 17-year study of the Cottonwood Lake wetland complex in North Dakota in the perspective of longer term measured and proxy hydrological records. *Climat. Change* 40, 189–209. <https://doi.org/10.1023/A:1005448416571>

Wolfe, B.B., Karst-Riddoch, T.L., Hall, R.I., Edwards, T.W., English, M.C., Palmi, R., McGowan, S., Leavitt, P.R., Vardy, S.R., 2007. Classification of hydrological regimes of northern floodplain basins (Peace–Athabasca Delta, Canada) from analysis of stable isotopes ($\delta^{18}\text{O}$, $\delta^2\text{H}$) and water chemistry. *Hydrol. Process.* 21, 151–168. <https://doi.org/10.1002/hyp.6229>

Wood, S.N., 2011. Fast stable restricted maximum likelihood and marginal likelihood estimation of semiparametric generalized linear models. *J. Roy. Stat. Soc. B Stat. Methodol.* 73, 3–36. <https://doi.org/10.1111/j.1467-9868.2010.00749.x>

Wood, S.N., Pya, N., Säfken, B., 2016. Smoothing parameter and model selection for general smooth models. *J. Am. Stat. Assoc.* 111, 1548–1575. <https://doi.org/10.1080/01621459.2016.1180986>

Yi, Y., Falcone, M.D., Edwards, T.W., Brock, B.E., Wolfe, B.B., 2008. A coupled isotope tracer method to characterize input water to lakes. *J. Hydrol.* 350, 1–13. <https://doi.org/10.1016/j.jhydrol.2007.11.008>

Zăvoianu, I., 1985. *Morphometry of Drainage Basins. Developments in Water Science* 20. Elsevier, New York. 238 pp

Zongxing, L., Qi, F., Wang, Q., Song, Y., Aifang, C., 2016. Contribution from frozen soil meltwater to runoff in an in-land river basin under water scarcity by isotopic tracing in northwestern China. *Glob. Planet. Change* 136, 41–51. <https://doi.org/10.1016/j.gloplacha.2015.12.002>

Table 1. Summary statistics for isotope mass balance results, catchment characteristics, and land use for all study lakes.

Lake/ Catchment Characteristic	Mean	Standard	Median	Median
--------------------------------	------	----------	--------	--------

		deviation		absolute deviation
E/ I (%)	32.2	15.9	29.7	17.1
Runoff Coefficient (%)	22.1	45.9	6.9	8.8
Water Yield (mm yr ⁻¹)	100.8	181.0	35.5	45.0
Drainage Basin Ratio	0.4	0.3	0.3	0.3
D-excess (‰)	-16.3	6.6	-16.6	7.1
Hydraulic Conductivity (cm h ⁻¹)	9.1	9.3	5.4	2.5
Sand content (% mass)	45.1	15.0	44.0	8.9
Average Distance Between Streams (m)	101.9	57.9	101.0	71.2
Average Distance of Overland flow (m)	88.5	60.3	87.0	81.5
Drainage Density (km ⁻¹)	0.4	0.4	0.3	0.3
Sink Volume (m ³ x10 ⁸)	2.9	8.0	2.9	0.4
Form Factor	0.3	0.1	0.3	0.11
Winter Precipitation (mm)	205.5	89.9	211.0	79.6
Summer Precipitation (mm)	266.3	35.1	256.8	28.5
Evaporation (m)	0.8	0.09	0.8	0.09
Lake Max Depth (m)	6.5	6.3	4.00	4.00
Lake Surface Area (m x10 ⁷)	1.9	6.5	0.4	0.4
Crop cover (% catchment)	46.9	27.5	52.6	30.1
Tree cover (% catchment)	6.1	14.6	1.2	1.7
Wetland cover (% catchment)	3.3	7.7	2.0	1.7
Urban cover (% catchment)	0.9	2.1	0.4	0.5
Grass cover (% catchment)	28.1	22.1	22.0	20.4

1086 Table 2. Fit statistics for generalized additive models (GAM) used for spatial analysis of meteorological and isotope-inferred
 1087 hydrological parameters.

Variable	Deviance Explained (%)	F-statistic*	df	p
Winter Precipitation (SWE)	91.6	23.7	34.6	<<0.001
Evaporation	94.7	25.7	44.6	<<0.001
Precipitation Deficit	95.4	33.3	42.4	<<0.001
δI	30.5	6.5	6.2	<<0.001
E/ I	40.2	3.1	18.5	0.0001
D-excess	51.8	3.5	21.9	<<0.001
Runoff	43.8	2.1	20.0	0.008
Water Yield - GDA	31.8	1.4	19.6	0.1
Water Yield - SFDA	26.6	1.9	12.8	0.04
Runoff Coefficient - GDA	32.8	1.3	18.9	0.2
Runoff Coefficient - SFDA	26.6	2.8	9.6	0.004
Ungauged flow	43.8	2.1	20.0	0.009
Drainage Density- GDA	64.1	3.8	30.9	<<0.001
Sand Content - GDA	51.3	2.8	25.2	0.0001
Percent Crop - GDA	68.2	84.6*	22.6	<<0.001
Percent Grassland - GDA	53.4	44.5*	13.8	<<0.001

1088 * = chi-squared statistic for % cropland and % grassland.

1089 **Figure captions**

1090 Figure 1. Geographic locations of 105 study sites (red circles) sampled in southern Saskatchewan
1091 (main panel) in Canada (inset) during mid-July to mid-August 2013. Major waterbodies in the
1092 Saskatchewan marked in blue, with urban centres of Regina and Saskatoon in black stars. Total
1093 survey area was ~285,000 km². **Colour figure.**

1094 Figure 2. A) Isotope values plotted for all lakes with the local meteoric water line (LMWL) from
1095 Saskatoon, Saskatchewan, Canada. The local evaporative line (LEL) was calculated using mean
1096 conditions from Saskatoon and represents the general trajectory of lake isotope values from the
1097 weighted average precipitation value due to evaporation. Colours of the points represent the
1098 evaporation to inflow ratio of the lakes. B) the relative abundance of lakes that were categorized
1099 as rain (blue) vs winter (yellow) or mixed/intermediate precipitation (green) estimated from
1100 inflow isotope values (δ_i). **Colour figure.**

1101 Figure 3. Kernel density plot of lakewater $\delta^{18}\text{O}$ observations for precipitation from Saskatoon,
1102 SK, Canada (blue, yellow) and the inflow isotopic values, δ_i (pink), from the 105 lakes in 2013.
1103 Solid lines represent the mean values for snow and rain respectively with the dotted line noting
1104 the intersection between the distributions of rain and snow. **Colour figure.**

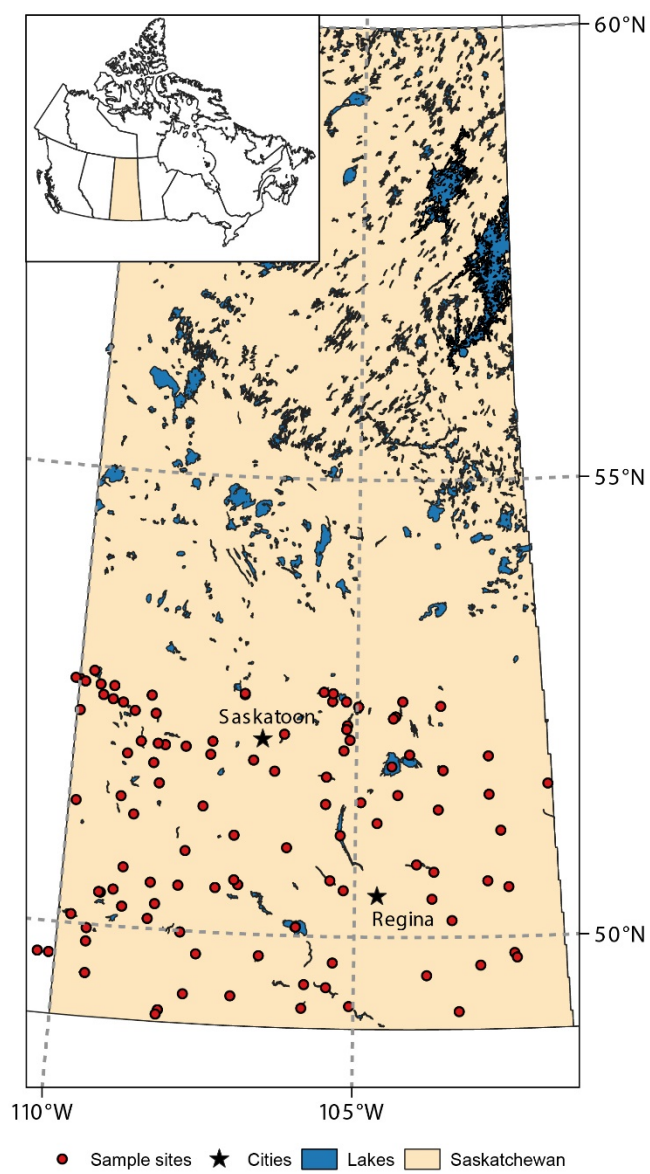
1105 Figure 4. Frequency histograms and boxplots of isotopic and estimated hydrological parameters
1106 for 105 prairie lakes surveyed during 2013. Panels include: (a) inflow oxygen isotope values
1107 (‰); (b) isotope mass balance estimates of evaporation/inflow ratios (E/I, %); (c) water yield
1108 (mm year⁻¹) estimated using gross drainage area (GDA) of each lake; (d) runoff coefficient (%)
1109 based on GDA; (e) water yield (mm year⁻¹) estimated using sink-free drainage area (SFDA); (f)

1110 runoff coefficient (%) based on SFDA. Boxplots of each parameter shows median, upper (75%)
1111 and lower (25%) quantile, $1.5 \times$ interquartile range, and outlier values. **Greyscale figure.**

1112 Figure 5. Spatial distribution of isotope mass balance results in southern Saskatchewan, Canada,
1113 during late-summer 2013. Panels include: (a) inflow oxygen isotope values (‰); (b) isotope
1114 mass balance estimates of evaporation/inflow ratios (E/I, %); (c) water yield, WY, (mm year^{-1})
1115 estimated using gross drainage area (GDA) of each lake; (d) runoff coefficient, C, (%) based on
1116 GDA; (e) water yield (mm year^{-1}) estimated using sink-free drainage area (SFDA); (f) runoff
1117 coefficient (%) based on SFDA, and; (g) estimated volume inflow water ($\text{m}^3 \times 10^6$). **Colour**
1118 **figure.**

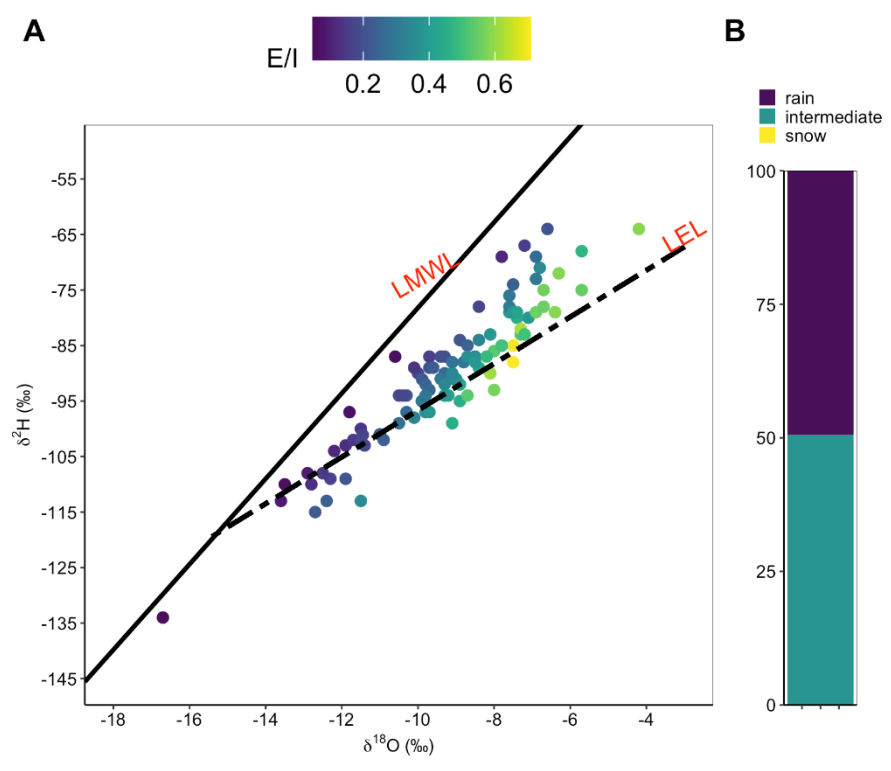
1119 Figure 6. Principle components analysis biplot of isotope-inferred hydrological features (bold),
1120 limnological features, and catchment characteristics based on the gross drainage area (GDA) of
1121 105 prairie lakes surveyed during late-summer 2013. Colours of site markers indicate the runoff
1122 coefficient. Land cover is expressed as % of the GDA associated with grass, trees, wetlands, and
1123 crops. Relative importance of sandy soils is also presented as % GDA. **Colour figure.**

1124



1125 Figure 1.

1126



1128

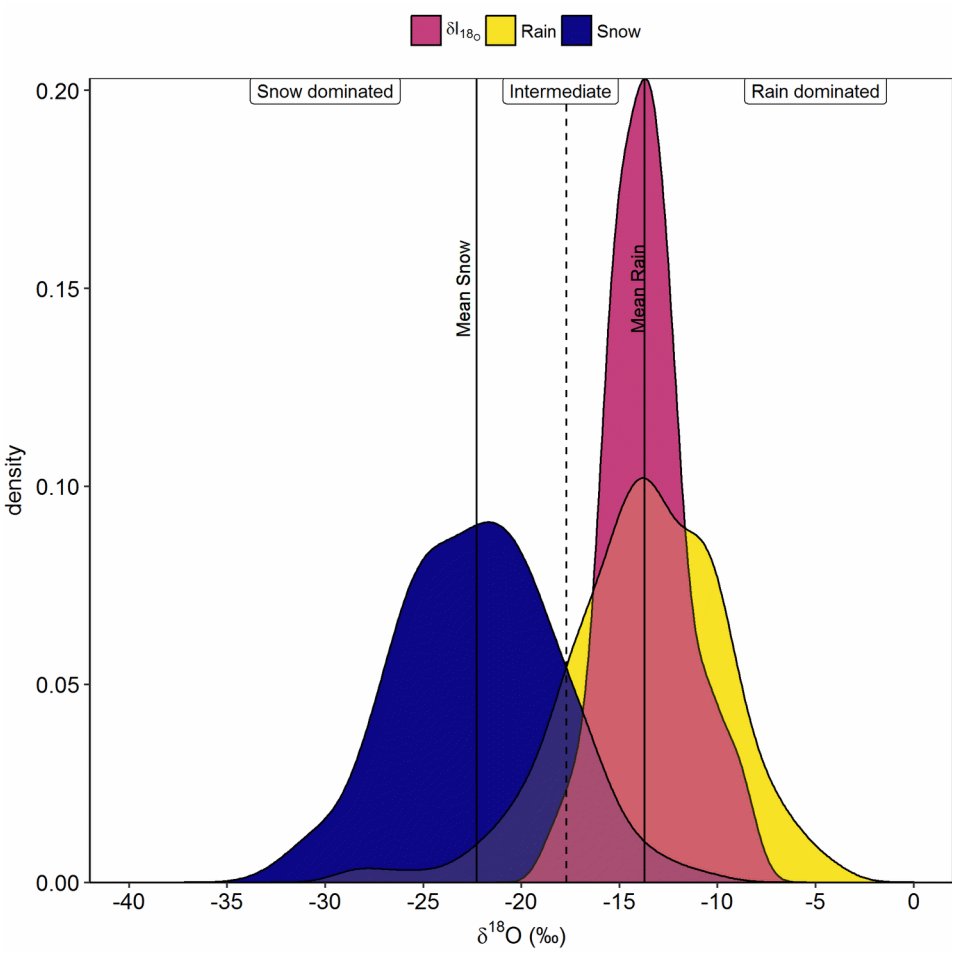
1129

1130 Figure 2.

1131

1132

1133

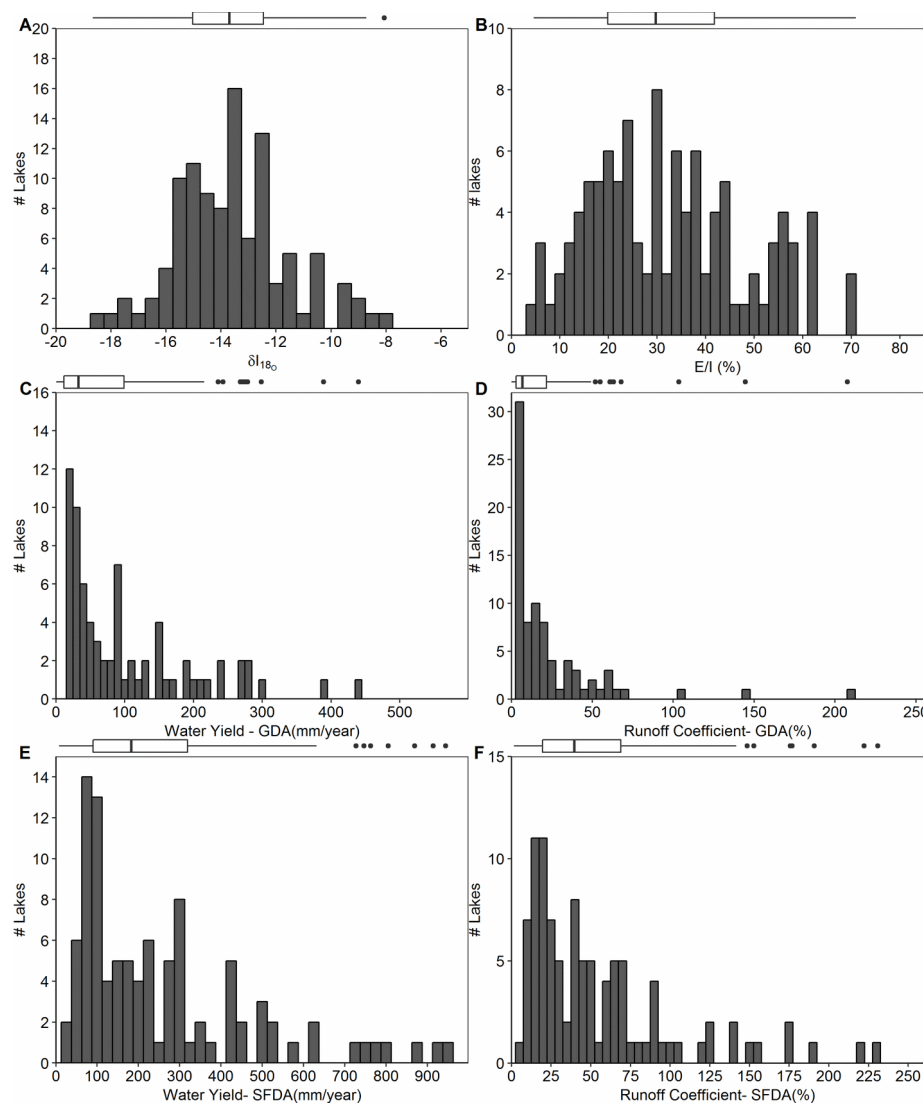


1135 Figure 3.

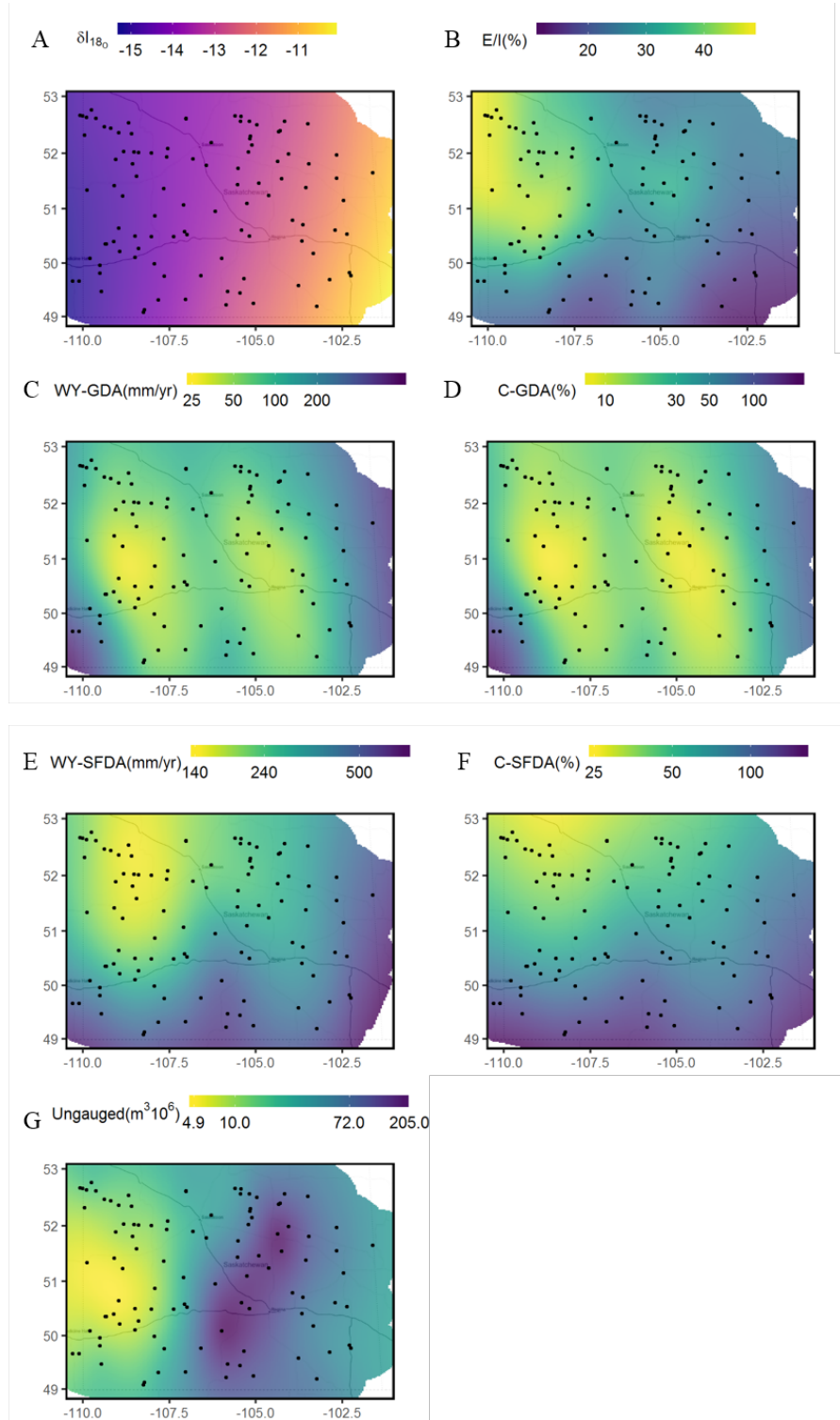
1136

1137

1138

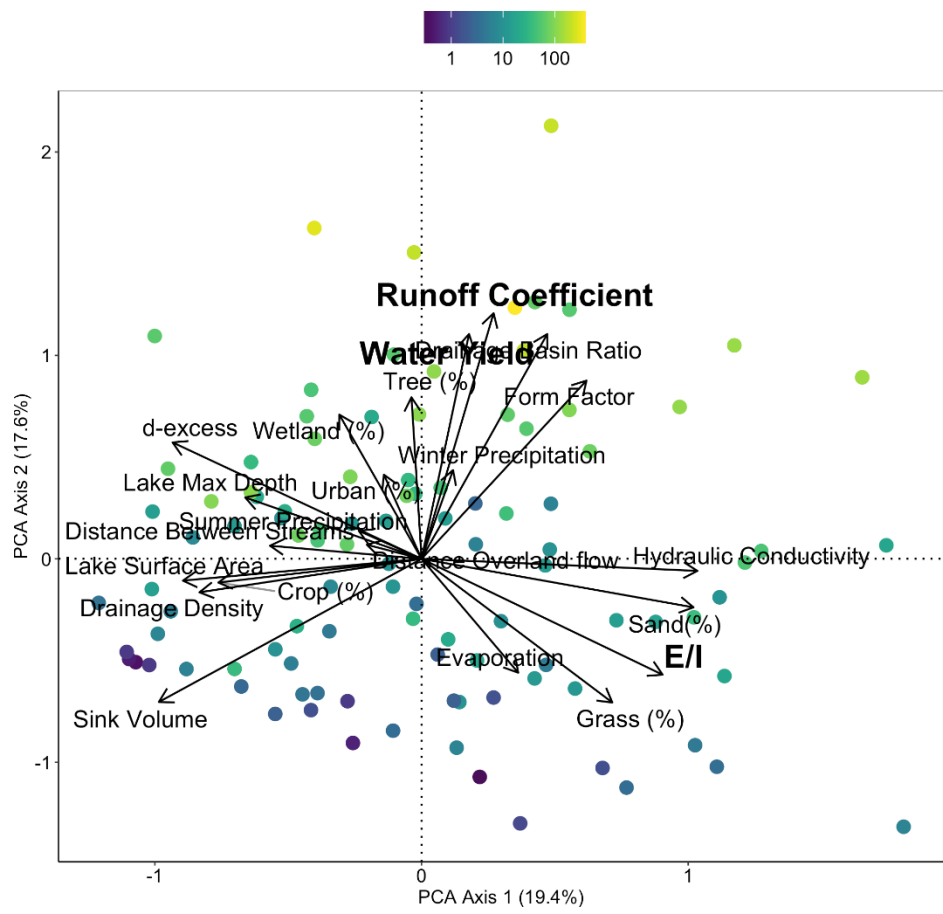


1140 Figure 4



1142 Figure 5.

1143

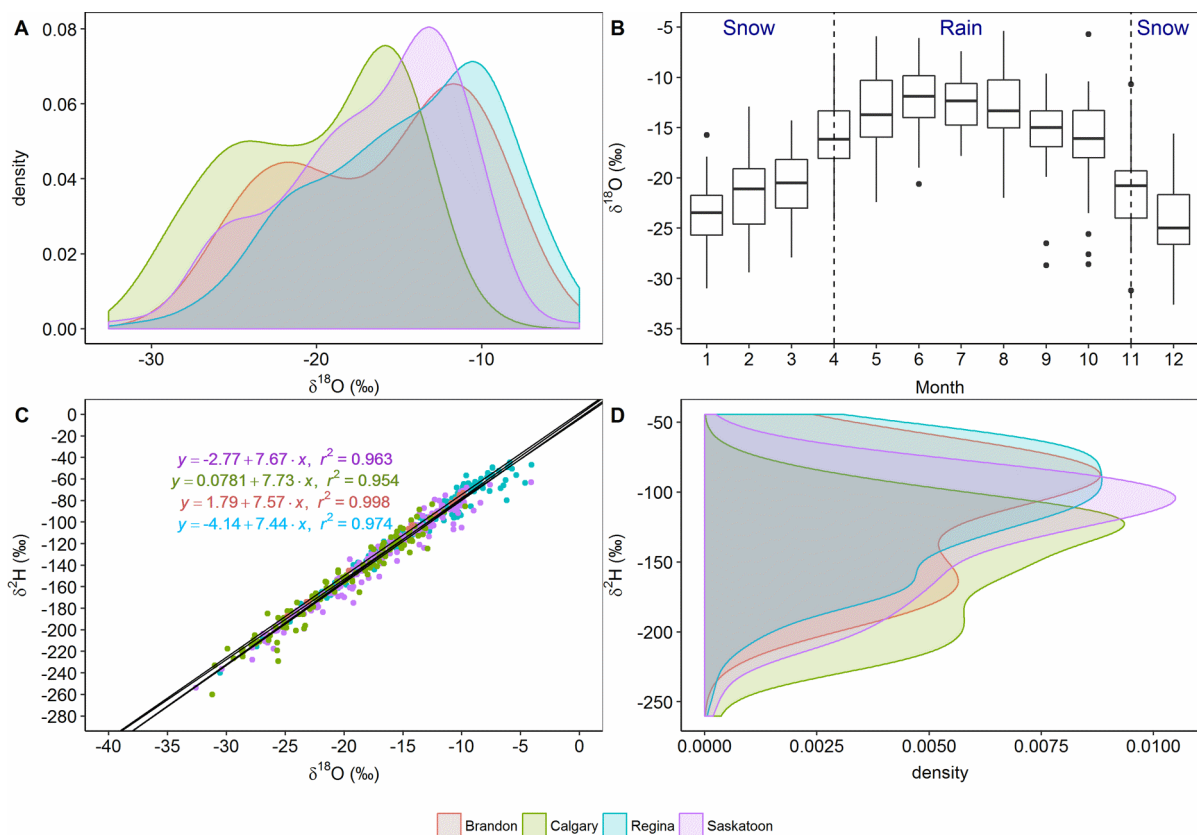


1145

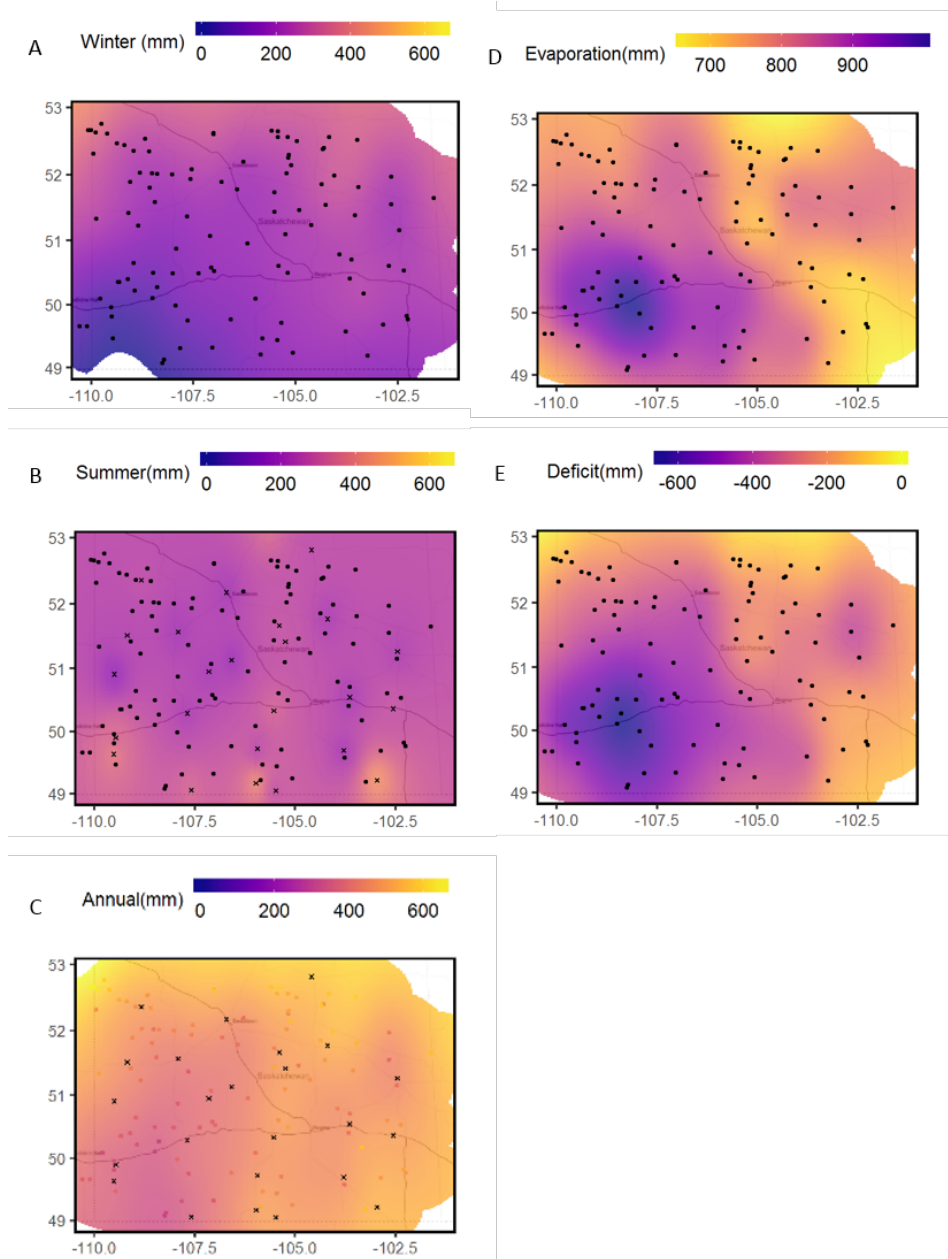
1146

1147

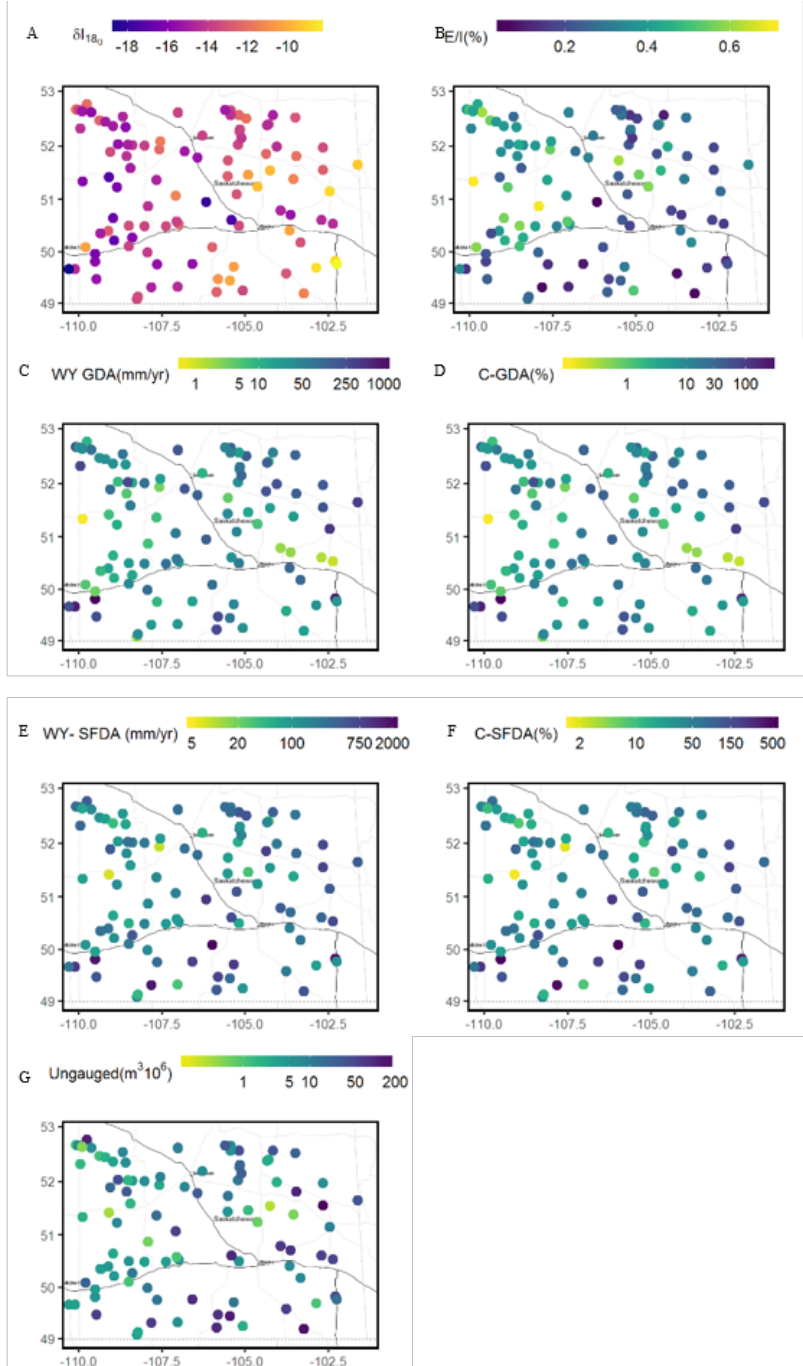
1148 Figure 6.



Supplementary Fig. 1. Comparison of isotopes in precipitation from sites within the study area as well as other locations on the Canadian Prairies, including southern (blue) and central Saskatchewan (purple), southern Manitoba (pink), and southern Alberta, Canada (green). Density plots of (a) $\delta^{18}\text{O}$ ‰, and (d) $\delta^2\text{H}$ ‰ suggest a bimodal distribution at all four locations, with (c) a common relationship among isotopes at all sites (local meteoric water line). Boxplots (b) of precipitation from Saskatoon, SK, Canada data increase during summer months associated with rain and decrease during periods of snow accumulation.



Supplementary Fig. 2. Maps of meteorological conditions for the 2013 hydrological year (November 2012 - October 2013) across the Saskatchewan study region smoothed using general additive models (GAM) and inverse distance weighting (IDW). Lake locations are noted with filled circles and climate stations with "x". Panels include: (a) snow water equivalent (SWE) of winter precipitation (mm) from the gross drainage basin (GDA); (b) summer precipitation (mm) gathered from Environment and Climate Change Canada gauging stations and interpolated using IDW; (c) annual precipitation (mm) as the sum of winter and summer precipitation; (d) estimated annual evaporation using the Meyer's method (Martin, 2002), and; (e) annual precipitation deficit (mm) estimated using the sum of precipitation minus potential evaporation, with negative values suggesting locations where evaporation exceeded precipitation.



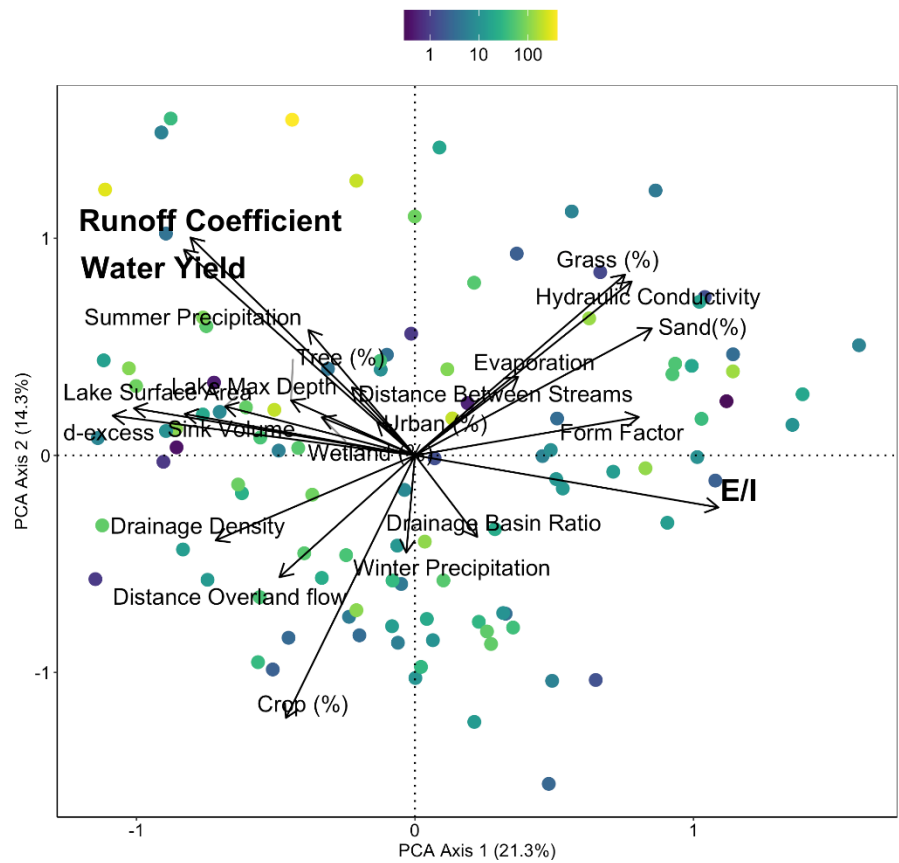
1168

1169 Supplementary Fig. 3. Site-specific data used in the spatial analysis in Figure 5. Panels include:
 1170 (a) inflow isotopic values (‰); (b) evaporation to inflow (E/I) ratio as (%); (c) water yield (WY)
 1171 calculated using the gross drainage area (GDA) (mm year⁻¹); (d) runoff coefficient (C) calculated
 1172 using the GDA (%); (e) WY calculated using the Sink Free Drainage Area (SFDA) (mm year⁻¹);
 1173 (f) C calculated using the SFDA (%), and; (g) isotope-inferred volume of ungauged flow (m³
 1174 x10⁶).

1175

1176

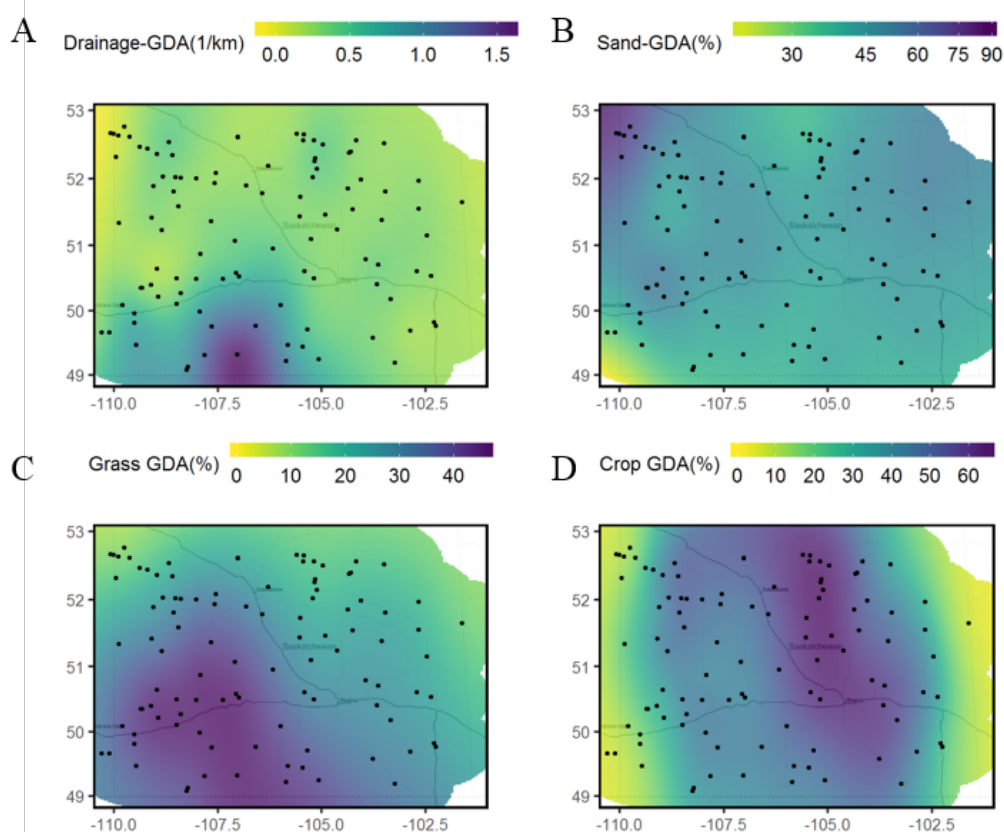
1177



1179 Supplementary Fig. 4. Principle components analysis of isotope mass balance inferred hydrology
1180 (bold), limnological features, and catchment characteristics estimated using the Sink Free
1181 Drainage Aarea (SFDA) of 105 prairie lakes surveyed during late-summer 2013. Colours of site
1182 markers indicate the runoff coefficient. Land cover is expressed as % of the GDA associated
1183 with grass, trees, wetlands, and crops. Relative importance of sandy soils is also presented as %
1184 GDA.

1185

1186

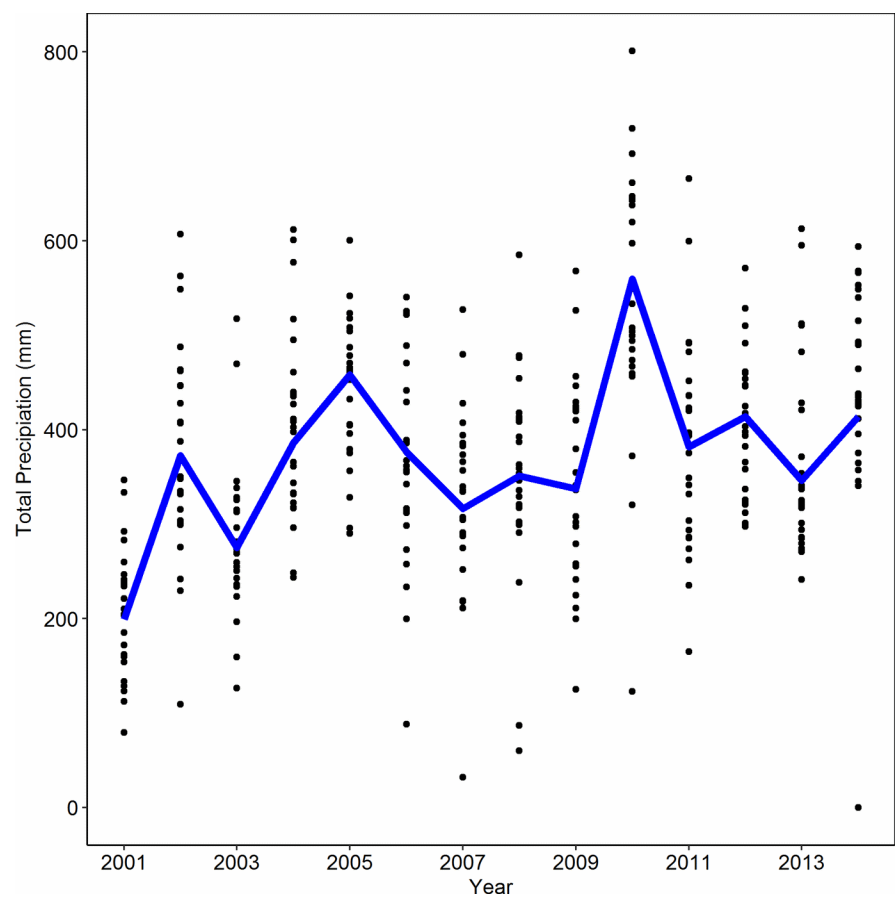


1187

1188

1189 Supplementary Fig. 5. Spatial distribution of proposed catchment drivers of lake water balance
 1190 including (a) drainage density (km^{-1}) within the gross drainage area; (b) percent (%) sand in soils;
 1191 (c) relative vegetation cover (%) that is grasses, and; (d) relative (%) land cover that is crop
 1192 agriculture. All spatial interpolation was completed using generalize additive models. See
 1193 Methods for details.

1194



1196 Supplementary Fig. 6. Total annual precipitation (mm; blue line) from all Environment and
1197 Climate Change Canada stations (black circles) within the study area from 2001-2014.